

Quantification of radio- photoluminescence glass dosimeter with different radionuclide beams

DH Seepamore



Orcid.org 0000-0001-8588-8253

Mini-dissertation submitted in partial fulfilment of the requirements for the degree *Master of Science in Applied Radiation Science* at North-West University

Supervisor: Prof M Mathuthu

Co-supervisor: Mr TG Kupi

Examination: May 2021

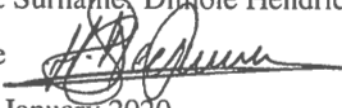
Student number: 18029701

DECLARATION

I herein declare that this mini-dissertation “Characterization of radio-photoluminescence glass dosimeter with different radionuclide beams” is the true demonstration of my own original research study and it has never been submitted for any degree at any university. Furthermore, I declare that contributions from other sources are evidently acknowledged by the indicated references.

Names & Surname: Dithole Hendrick Seepamore

Signature



Date: 10 January 2020

ACKNOWLEDGEMENT

I give thanks to God through His Holy Spirit which has provided me with strength of persistence and courage to finally conclude this beautiful piece of research which because of it, I had many sleepless nights. Words will never be sufficient enough to thank Prof Manny Mathuthu who throughout this research study has displayed enough supervision and endless support. He made time to travel to NMISA in Pretoria where I was taking research measurements to provide me with supervision. I want to thank Tebogo Kupi and Vincent Maselesele for the part he played on my research study.

To my loving Rakgadi Ipeleng Letsholo, I want to thank you for your selfless support and teachings that you have imparted to me throughout my upbringing. There are only few people that have a heart like yours. Moreover, I am thankful to my cousin brother Buti Maarohanye for your endless motivation and courage which you continuously injected in my life and for being my best friend and brother.

A special thanks to my kids; Resego, Kesego and Amogelang for continuously making me the happiest father alive. I will forever love you and cherish you as the gift that comes from God. I trust you will draw strong motivation from your father for his accolades and believe that nothing is impossible when faith meet commitment. I also want to extend my gratitude to my two families; Seepamore and Letsholo's family for parenting and supporting me throughout my upbringing.

If it was not because of NMISA for availing resources during the duration of my studies, this research study could have not been possible. I sincerely thank everyone at NMISA that supported my studies. Moreover, my gratitude goes to my special colleagues; Sonwabile Ngcezu, Refuoe Pepenene and Nkosi Maphumulo for their selfless support and guidance on this research study.

ABSTRACT

Human beings, animals, and the environment need to be protected against natural radiation sources and man-made radioactive materials. Radiation detectors are pivotal instruments in detecting radiation, be it personal exposure or environmental exposure. Now, valid calibrated radiation detectors are even more important to show accurate the response of the instruments to radiation. Thus, this information can be used to take necessary measures that should be implemented in case of high exposure risk detected to reduce radiation exposure levels to as low as reasonably achievable (ALARA). Radiophotoluminescence glass dosimeters (RPLGDs) are part of the luminescence family of dosimeters just like the Thermoluminescence dosimeters (TLDs). For years now, Panasonic thermoluminescence dosimeters have been used for both personal monitoring and environmental monitoring in South Africa and have limitations. TLDs are used to monitor different types of radiations. The quantity which is measured when TLDs are used for personal monitoring is personal dose equivalent, and for environmental monitoring is ambient dose. Thus, the same techniques as TLDs can be explored with RPLGDs since they both use the thermoluminescence phenomenon.

Three radiation sources (i.e. Cs-137, Co-60 & Am-241) were used to characterize the response of RPLGDs when exposed to different radiation doses. The ability of RPLGDs to be read more than once without losing original signal was studied. RPLGDs were investigated for their ability to measure both personal and environmental monitoring. Substitution method was used to determine the reference measurements on all radiation source setups. Reference detectors were positioned in the radiation beam to measure prescribed doses at the calculated time obtained from the dose rate and prescribed doses. Three radiation detectors (i.e. cylindrical ionization chamber, farmer ionization chamber and RPLGDs) were used. Two ionization chambers were used as reference detectors and RPLGDs as the unit under test (UUT) on each radiation source setup. Dose rates were used to determine the time of the prescribed radiation doses. RPLGDs were exposed to the same time as the reference detectors to accumulate radiation signal which was corrected to determine the absorbed dose. All the corrections that affected the response of UUT were implemented on the final readings of the RPLGDs to compare with the prescribed dose.

Table of contents

1 CHAPTER 1	1
1.1 Introduction	1
1.2 Problem statement	2
1.3 Research aim and objectives	2
1.3.1 Aim	2
1.3.2 Objectives	3
2 CHAPTER 2: LITERATURE REVIEW	4
2.1 Introduction	4
2.2 Basic concept of luminescence dosimetry	4
2.2.1 Luminescence	4
2.2.2 Radio-photoluminescence glass dosimeter (RPLGD)	5
2.2.3 Thermoluminescence dosimeter (TLD)	6
2.2.4 Optical stimulated luminescence dosimeter (OSLD)	8
2.3 RPLGD measuring principle	9
2.4 Silver activated phosphate glass (PG:Ag) chemical attributes	11
2.5 Dosimetric qualities and units	12
2.5.1 Kerma (K)	12
2.5.2 Air kerma rate	13
2.5.3 Absorbed dose	13
2.5.4 Ambient dose equivalent	14
2.5.5 Personal dose equivalent	14
2.6 Ionization chamber dosimetry system	15
2.6.1 Chambers and electrometer	15
2.6.2 Cylindrical farmer ionization chamber	17
2.7 Spherical ionization chamber	18
3 CHAPTER 3: MATERIALS AND METHODS	20
3.1 Introduction	20

3.1	Environmental condition monitoring	20
3.1.1	Temperature and pressure.....	20
3.2	Charge measurements.....	21
3.2.1	Background charge for pre (Q_{pre}) and post (Q_{post}) irradiation	21
3.2.2	Corrected charge collected during irradiation.....	22
3.3	Chamber calibration coefficients.....	23
3.4	Dose rate equation	24
3.5	Irradiation time	24
3.6	Cylindrical ionization farmer chamber used in Co-60 source measurements	25
3.7	Co-60 radiation source	25
3.8	Set-up in the Co-60 source	25
3.8.1	Set-up of cylindrical ionization farmer chamber in Co-60 beam	25
3.8.2	Set-up of RPLGD in Co-60 beam.....	26
3.9	Spherical ionization chamber used in Cs-137 source measurements	27
3.10	Cs-137 radiation source.....	27
3.10.1	Set-up in the Cs-137 source.....	28
3.10.2	Set-up of spherical ionization farmer chamber in Cs-137 beam	28
3.10.3	Set-up of RPLGD in Cs-137 beam	29
3.11	Spherical ionization chamber used in Am-241 source measurements	29
3.12	Am-241 radiation source	29
3.13	Set-up in the Am-241 source.....	30
3.13.1	Set-up of spherical ionization chamber in Am-241 beam	30
3.13.2	Set-up of RPLGD in Am-241 beam.....	30
3.14	Prescribed doses used to irradiate RPLGD	31
3.15	Glass element	32
3.16	Loading the RPLDs using a tweezer or loading device.....	32
3.17	Annealing magazine and read-out magazine.....	33
3.18	Annealing and pre-heat oven.....	34

3.19	Dose Ace reader (FGD-1000)	35
3.20	Magazine correction factors	36
3.21	Sensitivity correction factors for glass dosimeters	36
3.22	Non-linearity and linearity correction factors	37
3.23	Calibration coefficient of RPLGD in Co-60 beam.....	38
3.24	Air kerma calibration coefficient of RPLGD in Cs-137 beam.....	38
3.25	Air kerma calibration coefficient of RPLGD in Am-241 beam	39
3.26	RPLGD absorbed dose	39
4	CHAPTER 4: RESULTS AND DISCUSSIONS	40
4.1	Introduction	40
4.2	Magazine correction factors	40
4.3	Environmental condition measurements	41
4.3.1	Temperature and pressure measurements	41
4.3.2	Correction factors for temperature and pressure.....	42
4.4	Charge measurements.....	42
4.4.1	Pre and post-irradiation charge measurements with cylindrical ionization farmer chamber in Co-60 beam	42
4.4.2	Pre and post-irradiation charge measurements with spherical ionization chamber in Cs-137 beam .	43
4.4.3	Pre and post-irradiation charge measurements with spherical ionization chamber in Am-241 beam.. .	44
4.4.4	Irradiation charge measurements in Co-60, Cs-137 and Am-241 source	44
4.4.5	Corrected charge measurements for Co-60, Cs-137 and Am-241 source.....	45
4.5	Dose rate results	46
4.5.1	Co-60 source dose rate.....	46
4.6	Irradiation time results.....	47
4.7	Radiation counts acquired by RPLGD	47
4.7.1	Co-60 source radiation counts	48
4.7.2	Cs-137 source radiation counts.....	48
4.7.3	Am-241 source radiation counts.....	49

4.8 Sensitivity Correction Factors of RPLGD.....	49
4.8.1 Sensitivity correction factors of RPLGD in Co-60 source	49
4.8.2 Sensitivity correction factors of RPLGD in Cs-137 source.....	50
4.8.3 Sensitivity Correction Factors of RPLGD in Am-241 source	50
4.9 RPLGD calibration coefficients	51
4.9.1 RPLGD calibration coefficient for Co-60 source	51
4.9.2 RPLGD calibration coefficient for Cs-137 source	52
4.9.3 RPLGD calibration coefficient for Am-241 source.....	53
4.10 Linearity correction factors for RPLGD.....	54
4.10.1 Linearity correction factors for RPLGD in Co-60 source	55
4.10.2 Linearity correction factors for RPLGD in Cs-137 source.....	56
4.10.3 Linearity correction factors for RPLGD in Am-241 source	57
4.11 RPLGD corrected radiation counts - absorbed dose	58
4.11.1 RPLGD Absorbed dose in Co-60 beam.....	58
4.11.2 RPLGD Absorbed dose in Cs-137 beam.....	59
4.11.3 RPLGD absorbed dose in Am-241 beam	60
5 CHAPTER 5: CONCLUSION	62
5.1 Annexure 1	64
5.2 Annexure 2	65
5.3 Annexure 3	67
5.4 Annexure 4	68
6 REFERENCES	69

List of Tables

Table 1: Conversion coefficients from air kerma to ambient dose equivalent	14
Table 2: Conversion coefficients from air kerma to personal dose equivalent rate	15
Table 3: Electrometer factor.....	23
Table 4: Calibration coefficients.	23
Table 5: Prescribed doses for the three sources.	31
Table 6: Temperature and pressure for radiation sources.	41
Table 7: Correction factors for temperature and pressure for three sources.	42
Table 8: Leakage measurements for Co-60 source.	42
Table 9: Leakage measurements for Cs-137 source.....	43
Table 10: Leakage measurements for ^{241}Am source.	44
Table 11: Irradiation charge measurements for Co-60, Cs-137 and Am-241 source.	45
Table 12: Charge measurements	46
Table 13: Source dose rates.....	46
Table 14: Irradiation times and corresponding prescribed doses.....	47
Table 15: RPLGD calibration coefficient in ^{60}Co source.	51
Table 16: RPLGD calibration coefficient in ^{137}Cs source.	52
Table 17: RPLGD calibration coefficient in ^{241}Am source.....	53
Table 18: Corrected radiation counts by Co-60 source.....	58
Table 19: Corrected radiation counts by Cs-137 source.	59
Table 20: Corrected radiation counts by Am-241 source.	60
Table 21: Magazine correction factors.....	64
Table 22: Co-60 results.	65
Table 23: Co-60 results.	66
Table 24: Cs-137 results.....	67
Table 25: Am-241 result.	68

List of Figures

Figure 1: A schematic energy level diagram showing (a) the excitation and relaxation of an electron in fluorescence and (b) the excitation, trapping, releasing and relaxation of an electron in phosphorescence. G represents the ground state, E represents an excited state and M a metastable state (Kristina Jorkov, 2004).	5
Figure 2: TLD reader (Joanna & Govinda, 2005).	7
Figure 3: A schematic diagram of the energy levels of a crystalline material that sustains thermoluminescence or optical luminescence. The numbers in the diagram represent the following: 1 is the absorption of radiation and subsequent charge separation; 2 is the migration and trapping of an electron, after charge separation; 3 is the migration and trapping of an hole, after charge separation; 4 is a moderately deep electron trap; 5 is a moderately deep hole trap; 6 is a very deep electron trap; 7 is a shallow electron trap; 8 is the ejection of an electron out of a trap by absorption of heat, thermoluminescence, or light, optical luminescence; 9 is the migration of the untrapped electron; 10 is the recombination of an electron and hole at a hole trap; 11 is the emission of light at a luminescence centre, which received energy from the recombination of the electron and hole.	9
Figure 4: Schematic diagram of RPL trap formation, excitation and fluorescence (Julian A, 1987).	10
Figure 5: The colour centres formation mechanism of FD7 (A.T.G) (David YC & Shing-Ming, 2011).	11
Figure 6: Electrometer in feedback mode of operation (Joanna & Govinda, 2005).	17
Figure 7: Basic design of a cylindrical farmer type ionization chamber (Joanna & Govinda, 2005).	18
Figure 8: Litre spherical ionization chamber (Joanna & Govinda, 2005).	19
Figure 9: Ionization farmer chamber set-up in the Co-60 source.	26
Figure 10: RPLGD set-up in the Co-60 source.	27
Figure 11: Spherical ionization chamber set-up in ¹³⁷ Cs source.	28
Figure 12: RPLGD set-up in the ¹³⁷ Cs source.	29
Figure 13: Spherical ionization chamber set-up in ²⁴¹ Am source.	30
Figure 14: RPLGD set-up in ²⁴¹ Am source.	31
Figure 15: Reading centre point and reading range of glass dosimeter (LTD AGC TECHNO GLASS CO, 2008).	32
Figure 16: (a) loading device and (b) tweezer.	33
Figure 17: Magazine reader and annealing magazine.	34
Figure 18: Annealing and pre-heating oven.	35

Figure 19: Dose ace reader FGD-1000.	36
Figure 20: Magazine correction factors for actual data, correction factors and curve fitting.	40
Figure 21: Co-60 source irradiation counts measured by RPLGD.	48
Figure 22: Cs-137 source irradiation counts measured by RPLGD.	48
Figure 23: Am-241 source irradiation counts measured by RPLGD.	49
Figure 24: Sensitivity correction factors of RPLGD in Co-60 beam.	49
Figure 25: Sensitivity correction factors of RPLGD in Cs-137 beam.	50
Figure 26: Sensitivity correction factors of RPLGD in Am-241 beam.	51
Figure 27: Non-linearity coefficients of RPLGD in ⁶⁰ Co beam.	55
Figure 28: Linearity correction factors of RPLGD in ⁶⁰ Co beam.	55
Figure 29: Non-linearity coefficients of RPLGD in ¹³⁷ Cs beam.	56
Figure 30: Linearity correction factors of RPLGD in ¹³⁷ Cs beam.	56
Figure 31: Non-linearity coefficients of RPLGD in ²⁴¹ Am beam.	57
Figure 32: Linearity correction factors of RPLGD in ²⁴¹ Am beam.	57
Figure 33: Absorbed dose by RPLGD in ⁶⁰ Co source.	58
Figure 34: Absorbed dose by RPLGD in ¹³⁷ Cs source.	60
Figure 35: Absorbed dose by RPLGD in ²⁴¹ Am source.	61

List of abbreviations

RPLGD – Radio-photoluminescence glass dosimeter
RPL - Radio-photoluminescence
TLD - Thermoluminescence dosimeter
OSLD - Optically stimulated luminescence dosimeter
ATGC - Asahi Techno Glass Corporation
KNRC - Karlsruhe Nuclear Research Centre
NMISA - National Metrology Institute of South Africa
IAEA - International Atomic Energy Agency
ICRU - International Commission on Radiation Units
PSL - Primary Standard Laboratory
SSD - Secondary Standard Laboratory
NPL - National Physical Laboratory
DSL - Dosimetry Standard Laboratory
BIPM - Bureau International des Poids et Mesures
PTW - Physikalisch-Technische Werkstätten GmbH
RAKR - Reference air kerma rate
PDE - Personal dose equivalent
ADE - Ambient dose equivalent
ISO - International Standard Organization
UV - Ultra-violet
PMT -Photomultiplier tube
PUV - Pulsed ultra-violet
ALARA - As low as reasonable achievable
Am-241 - Americium 241
Cs-137 - Caesium 137
Co-60 - Cobalt 60
Gy - Grey
Sv - Sievert
R – Roentgen

1 CHAPTER 1

1.1 Introduction

Ionizing radiation can be used as a useful technique yet has a potential of being vastly dangerous when it interacts with matter. It is harmful to living organisms, yet it can be used as a useful technique to cure cancerous cells (Hooshang, Shuzo, & Dimitris, 2012). To detect different types of radiation, different radiation instruments are used. Radiation can be deposited to matter in different radiation forms, e.g. gamma, x-ray, beta, alpha radiation and etc. In this study, the focus was primarily on the interaction of gamma radiation with luminescence material. The type of luminescent material that was under investigation in this study is called radio-photoluminescence glass dosimeter (RPLGD) which forms part of the family of other known passive dosimeters such as the thermoluminescence dosimeters (TLD) and the optical stimulated luminescence dosimeters (OSLD). This study explores the response of passive dosimeter's family, particularly RPLGD. The primary focus of the study was to characterize RPLGD with three radiation sources. For more than 50 years scientist have been working on the development of RPLGD which was first introduced in 1947 with a poor luminescence material and readout technique. In 1950, a new RPLGD was developed (glass compound as the luminescence material) to address the limitations of TLD. Pulsed ultra-violet (PUV) laser beam is used to excite the glass compound of the RPLGD which then emits an orange luminescence (Jeong-Eun, et al., 2009).

The excitation source was changed from ultra-violet (UV) light to a PUV laser beam. When a silver activated phosphate glass compound of the radio-photoluminescence (RPL) glass dosimeter is exposed to ionizing radiation, stable colour centres are formed, and the colour centres increases with increase in radiation intensity. The colour centres are excited after being irradiated by the PUV laser beam and emit orange light (Burgkhardt) of 600 nm to 700 nm. This phenomenon is called radio-photoluminescence (Miyamoto, et al., 2011). Radiation counts received by glass dosimeter is linearly proportional to the orange light emitted by the RPL glass dosimeter. Thus, RPL glass dosimeter's signal reading can be repeated unlimited times without losing the actual signal whereas TLDs can only be read once. TLDs are the most used traditional passive dosimeters in the radiation protection field for personal monitoring and environmental monitoring. However, TLD and OSLD have different excitation methods as well as the readout techniques. Most luminescence material that make up the solid structure of TLDs are phosphor in nature such as calcium fluoride (CaF) or lithium

fluoride (LiF). When radiation interacts with the solid crystal, it deposits energy to the phosphor and the material is ionized (Weihai, Weiqi, Guoying, & Gang, 2007). Energy deposited by radiation is retrieved by annealing the dosimeter which then excite the electrons to a higher state (excitation state). The excited electrons are then released to the ground state by releasing captured energy which is equivalent to the amount of absorbed dose received by the dosimeter. The challenge of the TLDs is, their inability to be read more than once without losing the initial signal, trapped radiation energy disappears after a single readout. Thus, the limitation of TLDs have always been a challenge in the radiation protection applications particularly when the radiation dose measurements need to be verified repeatedly. The study researches at one of the alternative passive dosimeters to address the TLDs challenged.

1.2 Problem statement

Thermoluminescent dosimeters are the most used personal dosimeters for radiation workers in South Africa and are recommended by the Department of Health (DoH) or the South African Health Products Regulatory Authority (SAHPRA). The limitation of TLDs is that, accumulated radiation signal disappears after being read once. Now in order to come up with the solution to the limitation of TLDs and to introduce a device that has a potential to be read more than once (to provide better statistical dose measurement) which can be used by all radiation workers in South Africa, RPLGDs were studied as an alternative. RPLGDs were characterized with three radiation sources (i.e. Cs-137, Co-60 & Am-241). The ability of RPLGDs to be read more than once without losing original signal was also studied by taking as many measurements to get better accuracy of the accumulated signal and reading glass dosimeter multiple times to obtain a better statistical average accuracy.

1.3 Research aim and objectives

1.3.1 Aim

To quantify the response of radio-photoluminescence glass dosimeter with different radionuclide sources.

1.3.2 Objectives

The objectives of this work were to:

- develop reference air kerma and absorbed dose to water measurements for RPLGDs with three radiation sources (i.e. Co-60, Cs-137 and Am-241 source).
- use the reference measurements for air kerma and absorbed dose to water as the baseline measurements for personal and environmental monitoring measurements by applying conversion factors of each radiation source.

2 CHAPTER 2: LITERATURE REVIEW

2.1 Introduction

Amongst the existing passive dosimeters, RPLGDs are the alternative dosimeters to use for personal and environmental monitoring radiation exposures and they have the ability to be read more than once as compared to the traditional TLDs. RPL glass dosimeter do not provide real time reading or radiation dose levels at an instant during exposure, however they have the advantages in a long term monitoring of personnel or environmental dose accumulation such as high sensitivity, low energy dependence, low fading effect and good dose linearity, capability of repeating readout, good physicochemical stability compared to TLD (Sijun, Chunlei, Dongbing, & Kefeng, 2011) and (Sato, et al., 2013). The PUV laser beam is a technique that is used to cause excitement of the silver ions in the glass material of the RPLGD which leads to the radiation absorbed to be read easily. Composition of the glass material of radio-photoluminescence material is of silver activated phosphate glass. RPL glass dosimeters exhibit RPL phenomenon when exposed to ionizing radiation (Yamamoto, 2011). Since the meaningful developments of the new RPL glass dosimeter of silver doped phosphate glass, scientist have been contributing significantly in the advancement of the RPL glass dosimeter (Lee, et al., 2009).

2.2 Basic concept of luminescence dosimetry

2.2.1 Luminescence

When ionizing radiation energy is absorbed by luminescence material, some of the energy is kept in metastable state. It is then released in the form of visible, ultraviolet or infrared light, the phenomenon is called luminescence (Podgorsak, 2008). Luminescence occurs as a result of light being released without the material undergoing any thermal process. It is the emission of light from any material and occurs from electronically excited state. Fluorescence and phosphorescence form the two categories of luminescence which are distinguished by the excited state (Lakowicz, 2013). Figure 1 illustrates the schematic energy level diagram of the excitation, releasing and relaxation of the electron in fluorescence and phosphorescence.

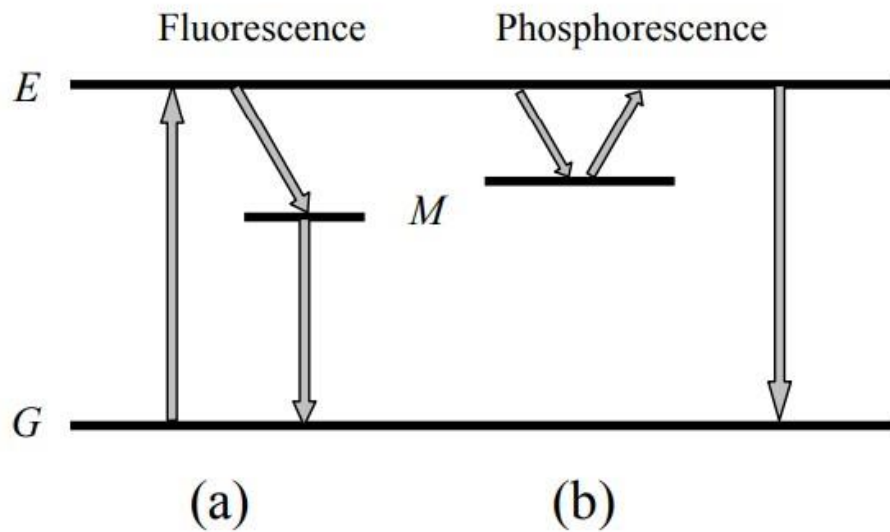


Figure 1: A schematic energy level diagram showing (a) the excitation and relaxation of an electron in fluorescence and (b) the excitation, trapping, releasing and relaxation of an electron in phosphorescence. G represents the ground state, E represents an excited state and M a metastable state (*Kristina Jorkov, 2004*).

2.2.2 Radio-photoluminescence glass dosimeter (RPLGD)

The use of radio-photoluminescence glass dosimeter for radiation measurements can be dated from the 1950s. During its initial development, it had a very poor measuring technique and high pre-dose. The RPL glass dosimeter is in constant development, and it is made of silver activated phosphate glass. A pulse ultraviolet laser is used to read the radio-photoluminescence from the glass dosimeter (Yohei, et al., 2008). The application of RPL dosimetry system is increasing in radiation protection field. Various RPL glass dosimeters are developed for different applications particularly for radiation protection measurements. When the glass dosimeter is exposed to ionising radiation, the luminescence material forms the colour centres. Fluorescence are emitted from the colour centres after the glass dosimeter is irradiated with pulsed ultraviolet laser. The orange luminescence is emitted when the glass compound is illuminated with ultraviolet rays. Thus, this process is called radio-photoluminescence phenomenon. The luminescence emitted is linearly proportional to the absorbed dose of ionizing radiation accumulated by radio-photoluminescence glass dosimeter (Lee, et al., 2009). New generation of RPL glass dosimeter was completed in 1990. The excitation source was changed from UV light into PUV beam (Huang & Shing-Ming, 2011). The interaction of ionizing radiation with glass dosimeter is shown in Figure 3 and the phases that takes place are RPL trap

formation, excitation and fluorescence. When radiation interact with a phosphor inside the glass material, trapped electrons are created and are metastable. Thus, post irradiation stimulated with light or optical radiation causes electrons in the metastable to move to an energy level above their post irradiation state and to return with the release of electromagnetic energy in the visible range.

Radio-photoluminescence glass dosimeters exhibit characteristics such as the following (Huang & Shing-Ming, 2011):

- Good reproducibility of the readout value.
- Long term stability of the fading effect less than 1 % (30 days).
- Low energy dependence for photons within ± 10 % (0.03 - 1.3 MeV).
- Good dose linearity of 0.01 - 500 mGy and
- Capability of repeating readout in the measurements of radiation dose.

2.2.3 Thermoluminescence dosimeter (TLD)

Thermoluminescence dosimeter is used for personal monitoring, environmental monitoring and medical dose verification. TLD monitoring systems were introduced in the late 1960 and during 1970s. In the next decades tremendous development took place worldwide in the field of thermoluminescence personnel dosimetry (Bhatt & Kulkarni, 2014). Thermoluminescence is one of the oldest applications that has been used in dosimetry field to measure accumulated dose due to external sources and for personal monitoring. Different materials are used that depicts thermoluminescence phenomenon, such as Ca:Mn, LiFi:Mg,Cu,P material used in lithium fluoride doped with Mg and Ti(LiFi:Mg,Ti). When TLD is irradiated or exposed to radiation, the crystal material traps the electron in metastable states. At room temperature, electron do not have sufficient energy to escape unless heat is applied on the material to promote electrons back to conduction band, where they will subsequently recombine with the hole (Seco, Clasie, & Partridge, 2014).

Point defects in the thermoluminescence materials created during crystal growth or solid-state sintering are able to trap electrons and holes generated during irradiation and this way can store

dosimetric information for a long time. To measure an accumulated dose, TL is heated in a reader and emits luminescent light amount which is proportional to absorbed dose. TLD is considered as a destructive technique, in that the signal is completely removed from the detector since readout require heating of the detector. Furthermore, it is slow and not suitable for high spatial resolution imaging (Akselroda, BZtter-Jensenb, & Mckeever, 2007). To reuse the dosimeter, the readings need to be annealed to a temperature of about 400 °C. A basic TLD reader system consists of a planchet for placing and heating the TLD, a photomultiplier tube (PMT) to detect the thermoluminescence light emission and convert it into an electrical signal linearly proportional to the detected photon fluence and an electrometer for recording the PMT signal as a charge or current. A basic schematic diagram of a TLD reader is shown in Figure 2 (Joanna & Govinda, 2005).

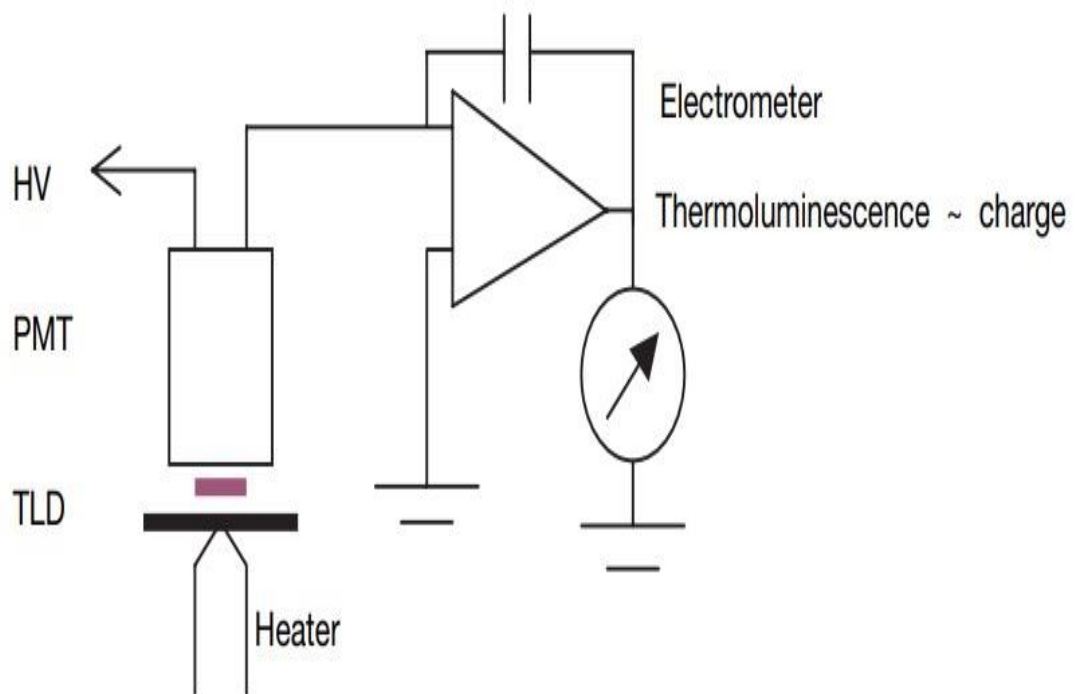


Figure 2: TLD reader (Joanna & Govinda, 2005).

For years now, Panasonic thermoluminescence dosimeters (TLDs) have been used for both personal monitoring and for environmental monitoring. TLDs are used to monitor X-ray, gamma, and beta radiation. The quantity which is measured when the TLDs are used for personal monitoring is personal dose equivalent, and for environmental monitoring is ambient dose in the environment. Regulations relating to group IV hazardous substance (Government notice R247 of 26 February 1993) is used as a guide for the dose limits. All radiation workers are legally required to be monitored, and TLDs are

recommended by the department of health as the radiation personal monitoring device. Thus, TLDs are passive dosimeters, and they provide accumulated radiation dose over time. TLDs have shortcomings that affect the consistency of retrieving the radiation signal acquired during the wearing period of the radiation workers and when used for environmental monitoring. They can only be read once, and the radiation signal disappears afterward. Furthermore, the TLDs are slow and not suitable for high spatial resolution imaging (Akselroda, BZtter-Jensenb, & Mckeever, 2007).

2.2.4 Optical stimulated luminescence dosimeter (OSLD)

Optical stimulated luminescence (OSL) is one of the many known stimulated phenomenon in science that can be induced by ionizing radiation and became a successful tool in radiation dosimetry. OSL utilizes materials and electronics and processes like thermoluminescence but interrogation of the detector is performed by photons instead of heat (Botter-Jensen, Mckeever, & Wintle, 2003). OSLDs are plastic disks infused with aluminium oxide doped with carbon ($A_3O_3:C$). These disks are encased in a light-tight plastic holder. Crystals of $A_3O_3:C$ when exposed to ionizing radiation store energy that is released as luminescence (420 nm) when the OSLD is illuminated with stimulation light (540 nm). The intensity of the luminescence depends on the dose absorbed by the OSLD and the intensity of the stimulation light. High sensitivity, precise delivery of light, fast readout times, simpler readers and easier automation are the main advantages of OSL in comparison with TLD. OSL allows for re-reads of the detector multiple times while maintaining the precision, and yet it still can be used as an erasable measurement technique. In comparison with thermoluminescence materials, OSL phosphors are not subjected to heating at high temperature, do not experience the so-called “thermal quenching effect”, and they can be mixed with or embedded in plastic (Akselroda, BZtter-Jensenb, & Mckeever, 2007) and (Kristina Jorkov, 2004). Figure 3 depicts a schematic diagram of the energy levels of a crystalline material that thermoluminescences or optical luminescence.

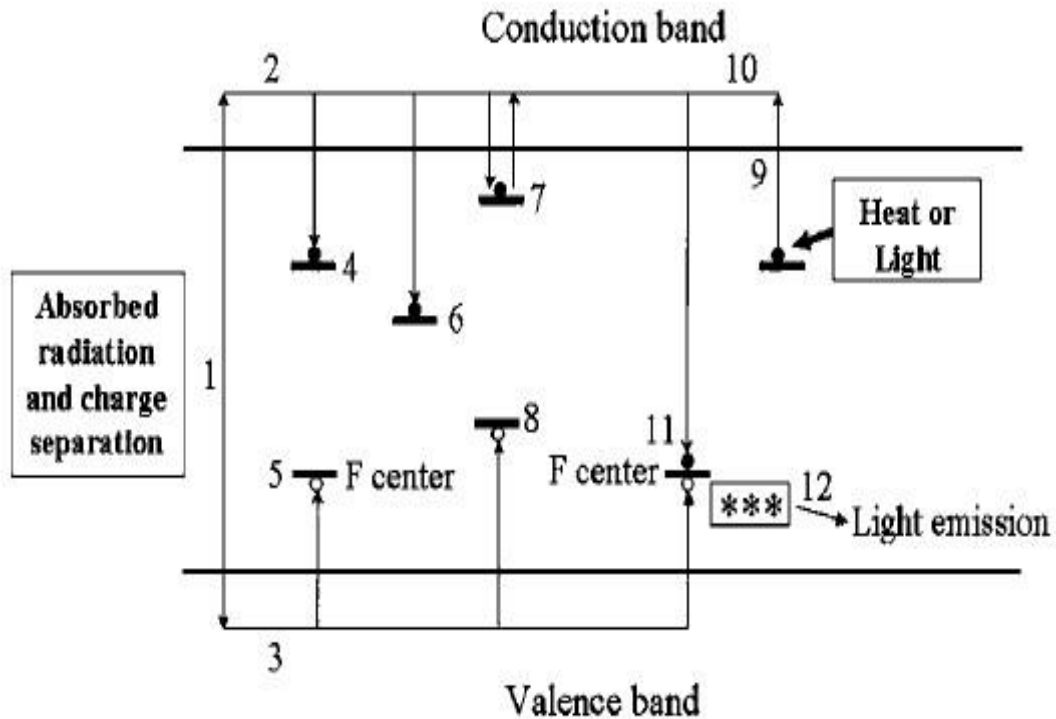


Figure 3: A schematic diagram of the energy levels of a crystalline material that sustains thermoluminescence or optical luminescence. The numbers in the diagram represent the following: 1 is the absorption of radiation and subsequent charge separation; 2 is the migration and trapping of an electron, after charge separation; 3 is the migration and trapping of a hole, after charge separation; 4 is a moderately deep electron trap; 5 is a moderately deep hole trap; 6 is a very deep electron trap; 7 is a shallow electron trap; 8 is the ejection of an electron out of a trap by absorption of heat, thermoluminescence, or light, optical luminescence; 9 is the migration of the untrapped electron; 10 is the recombination of an electron and hole at a hole trap; 11 is the emission of light at a luminescence centre, which received energy from the recombination of the electron and hole.

2.3 RPLGD measuring principle

When the glass compounds interact with radiation particles, the colour centres are formed. The colour centres release emission of light upon interacting with PUV laser beam. Consequently, the silver activated phosphate glass is excited by UV beam, and the glass emits an orange luminescence. Thus, this occurrence is named RPL. The quantity of luminescent which is discharged by the glass compound, is linearly proportional to the absorbed dose the glass dosimeter acquired (Jeong-Eun, et al., 2009) and (Huang & Shing-Ming, 2011).

The new development of the RPL glass dosimeter readout system was introduced in 1990 by Asahi Techno Glass Corporation (ATGC) in Japan and Karlsruhe Nuclear Research Centre (KNRC) in Germany (Huang & Shing-Ming, 2011). UV light was used as the old system to excite the glass compound, and the new development introduced PUV as the suitable technique that takes microseconds (s) (Toshio, et al., 2015). In addition to the rapid decline of the excitation time on the new development, the energy and positioning of the PUV beam can be precisely determined.

Figure 4 depicts the physical process that takes place when ionizing radiation interact with the glass material. The trapped electrons that are created when radiation interact with phosphor are metastable, so that post irradiation stimulation with light or optical radiation causes electrons in the trap to move to an energy level above their post irradiation state and to return to it with the release of electromagnetic energy in the visible range (Julian, 1987).

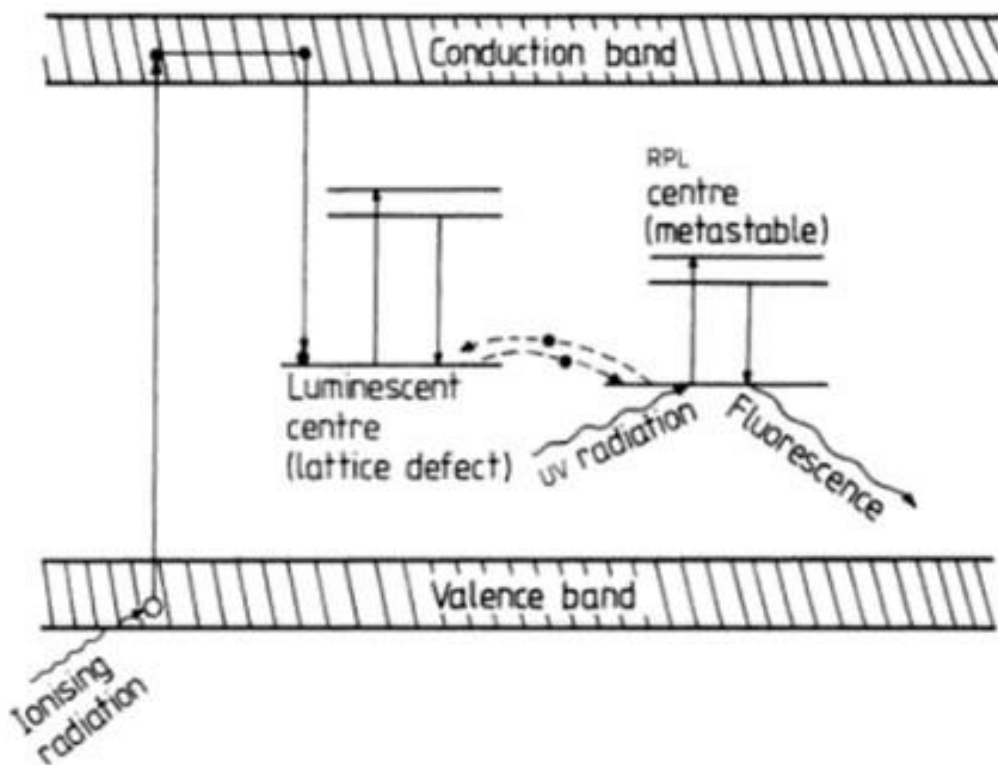


Figure 4: Schematic diagram of RPL trap formation, excitation and fluorescence (Julian, 1987).

2.4 Silver activated phosphate glass (PG:Ag) chemical attributes

The chemical structure of the AgPO_4 glass comprises of the colour centres which are well structured. The energy levels which are created by the colour centres of the AgPO_4 correlate to both the number of Ag^+ ions and of the trapped electrons. Thus, excessive numbers of ionic silver decrease the penetration efficiency of the PUV laser beam and increases energy dependence. Excitation efficiency and correct luminescence gives good balance ratio of Ag^+ ions in the chemical structure. The glass dosimeter which is usually used in the application of the RPL glass dosimeter for dose accumulation is FD-7. Electron hole pair are induced in the glass due to the interaction of ionizing radiation in the glass compound. This process results to electrons being apprehended into Ag^+ ions in the glass composition which leads to Ag^+ ions being transformed to Ag^0 ions (Hidehito, 1998). Ionizing radiation interact with PO_4 tetrahedron in glass, and it losses its electrons and traps positron holes hPO_4 . Simultaneously, the Ag^+ in glass traps a single electron and changes to the Ag^0 ion (Huang & Shing-Ming, 2011) as depicted in Figure 5 on the development mechanism of the colour centres formation.

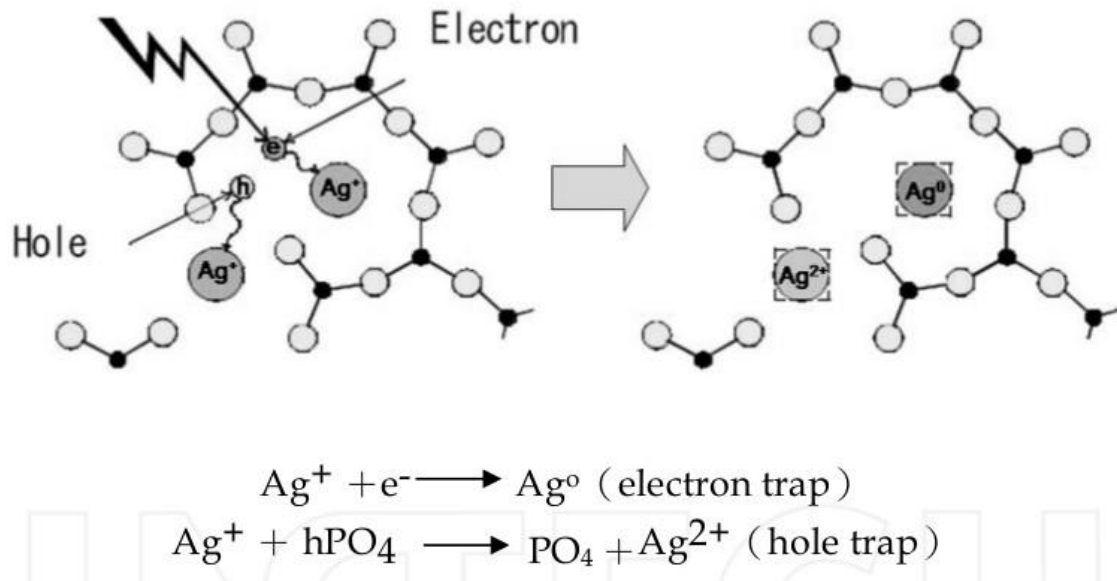


Figure 5: The colour centres formation mechanism of FD7 (A.T.G) (Huang & Shing-Ming, 2011).

The release of Ag^+ from the PG:Ag merges with free electrons (e^-) from PO_4^- and hPO_4 to form stable luminescence colour centres (Ag^0 and Ag^{++}). The colour centres get excited when irradiated by PUV laser beam of 337.1 nm. Electrons which are released by the colour centres; Ag^0 and Ag^{++} get excited to

higher energy level and visible orange light from 600 – 700 nm get emitted and it return to the ground state. However, the radiation imparted by the PUV beam to the electrons is not sufficiently adequate to allow electrons to be released from the colour centres. Glass dosimeter need to be heated at 400⁰C for one hour for electrons to gain sufficient energy to return to the valence band. The superior advantage of the glass dosimeter is that the colour centres do not disappear after readout technique, in fact the readout can be repeated unlimitedly (Huang & Shing-Ming, 2011)

2.5 Dosimetric qualities and units

2.5.1 Kerma (K)

Kerma is an acronym for kinetic energy released per unit mass. It is a non-stochastic quantity applicable to indirectly ionizing radiations such as photons and neutrons. It quantifies the average amount of energy transferred from indirectly ionizing radiation to directly ionizing radiation without concern as to what happens after this transfer. The energy of uncharged particles (photons) is imparted to matter in a two process. The photon radiation transfers energy to the secondary charged particles (electrons) through various photon interactions (the photoelectric effect, the Compton effect, pair production, etc) in the first stage. Thus, the charged particle transfers energy to the medium through atomic excitation and ionizations in the second stage (Joanna & Govinda, 2005).

Kerma for ionizing uncharged particles, is defined as the mean energy transferred from the indirectly ionizing radiation to charged particles (electrons) in the medium dE_{tr} per unit mass dm . Equation 1 is used to calculate kerma (K):

$$K = \frac{dE_{tr}}{dm} \quad (1)$$

Where dE_{tr} is the mean sum of the initial kinetic energies of all the charged particles liberated in a mass dm of a material by the uncharged particles incident on dm . The unit of kerma is joule per kilogram (J/kg). The name for the unit of kerma is the gray (Gy), where 1 Gy = 1 J/kg (Joanna & Govinda, 2005).

2.5.2 Air kerma rate

The rate at which energy is released as initial kinetic energies of all the charged ionizing particles which are released by uncharged ionizing particles (i.e. photons of energy $> \delta$) per unit mass of air (Nickovic & Adrovic, 2012). Equation 2 is used to calculate air kerma rate (\dot{K}_R)

$$\dot{K}_R = \frac{\Gamma_{\delta} A}{l^2} \quad (2)$$

Where Γ_{δ} is air kerma rate constant, l is a distance from a point source of activity A .

2.5.3 Absorbed dose

The absorbed dose is relevant to all type of ionising radiation fields, whether directly or indirectly ionising, as well as any ionising radiation source distributed within absorbing medium (Attix, 2008). The absorbed dose, D , is the quotient of $d\varepsilon$ by dm , where $d\varepsilon$ is the mean energy imparted by ionizing radiation to matter of mass dm (Gregoire & Mackie, 2011). The equation below is used to calculate the absorbed dose (D)

$$D = \frac{d\varepsilon}{dm} \quad (3)$$

The SI unit is J/kg and the special name is gray (Gy). The absorbed dose is derived from the mean value of the stochastic quantity of energy imparted and therefore does not reflect the random fluctuations of the interaction events in tissue. It is defined at any point in matter and, in principle, is a measurable quantity. Primary standards exist to determine the absorbed dose experimentally or by computation. The definition of absorbed dose has the scientific rigour required for a basic physical quantity. It implicitly takes account of the radiation field as well as of all of its interactions with matter inside and outside the specified volume. It does not, however, take account of the atomic structure of matter and the stochastic nature of the interactions.

2.5.4 Ambient dose equivalent

For the purposes of routine radiation protection, it is desirable to characterize the potential irradiation of individuals in terms of a single dose equivalent quantity that would exist in a phantom approximating the human body. The phantom selected is the so-called ICRU sphere made of 30 cm-diameter tissue-equivalent plastics with a density of 1 g/cm³ and a mass composition of 76.2 % oxygen, 11.1 % carbon, 10.1 % hydrogen and 2.6 % nitrogen. The “ambient dose equivalent”, $H^*(d)$, at a point in a radiation field is the dose equivalent that would be produced by the corresponding expanded and aligned field at a depth d in the ICRU sphere, on the radius opposing the direction of the aligned field. In an expanded field the fluence and its directional and energy distribution have the same values throughout the volume of interest as in the actual field at the point of reference. An expanded and aligned radiation field requires additionally that the fluence is unidirectional. For strongly penetrating radiations a reference depth, d , of 10 mm was recommended (Norbert, Hajek, & Berger, 2013).

To convert from air kerma to ambient dose equivalent, Table 1 depicts conversion coefficients for Co-60, Cs-137 and Am-241:

Table 1: Conversion coefficients from air kerma to ambient dose equivalent.

Radionuclide	$H^*(10)/K_a$
Co-60	1.16
Cs-137	1.20
Am-241	1.74

2.5.5 Personal dose equivalent

Personal dose equivalent, $H_p(d)$ (unit: sievert): The dose equivalent in ICRU tissue at an appropriate depth, d , below a specified point on the human body. The specified point is normally taken to be

where the individual dosimeter is worn. For the assessment of effective dose, Hp(10) with a depth $d = 10$ mm is chosen, and for the assessment of the dose to the skin and to the hands and feet the personal dose equivalent, Hp(0.07), with a depth $d = 0.07$ mm, is used. Personal dose equivalent is the operational quantity for individual monitoring (Martin, Harbison, Beach, & Cole, 2018).

To convert from air kerma to personal dose equivalent rate, Table 2 depicts conversion coefficients for Cs-137 and Am-241:

Table 2: Conversion coefficients from air kerma to personal dose equivalent rate.

Radionuclide	$H^*(10)/K_a$ Sv. Gy ⁻¹ (ISO 4037-3 Table 33)
Cs-137	1.20
Am-241	1.74

2.6 Ionization chamber dosimetry system

2.6.1 Chambers and electrometer

Ionisation chambers forms part of the family of the gas-filled detectors. It utilizes the simple principle of collecting the charge created by the interaction of incident radiation with electron in a volume of air. Ionisation chambers come in different forms depending on the specific requirements. They are used in different fields to determine the dosimetric quantities such as reference dose etc. The common properties of ionisation chambers regardless of the specific field where they are being utilized are as follows (Joanna & Govinda, 2005):

- An ionisation chamber is basically a gas filled cavity surrounded by a conductive outer wall and having a central collecting electrode. The wall and the collecting electrode are separated with a high-quality insulator to reduce the leakage current when a polarizing voltage is applied to the chamber.
- A guard electrode is usually provided in the chamber to further reduce chamber leakage. The guard electrode intercepts the leakage current and allows it flow to ground, bypassing the collecting electrode. It also ensures improved field uniformity in the active or sensitive volume of the chamber, with resulting advantages in charge collection.
- Measurements with open air ionisation chambers require temperature and pressure correction to account for the change in the mass of the air in the chamber volume, which changes with the ambient temperature and pressure.

Electrometers are devices for measuring different outputs of electrical and radiological measurements such as charge, current, absorbed dose to water, air kerma etc. An electrometer used in conjunction with an ionization chamber is a high gain, negative feedback, operational amplifier with a standard resistor or a standard capacitor in the feedback path to measure the chamber current or charge collected over a fixed time interval, as shown schematically in Figure 6 (Joanna & Govinda, 2005).

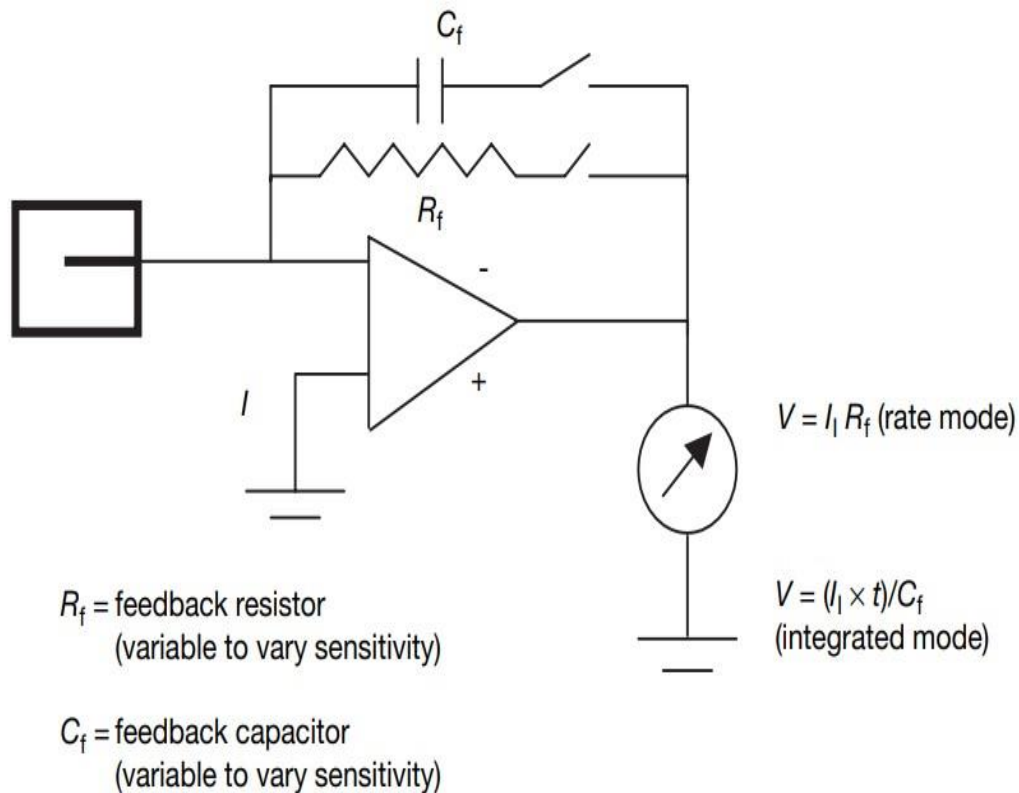


Figure 6: Electrometer in feedback mode of operation (Joanna & Govinda, 2005).

2.6.2 Cylindrical farmer ionization chamber

The cylindrical farmer chamber (model type 30012) has a sensitive volume of 0.6 cc and is intended for absolute dose measurements in radiation therapy. Correction factors needed to determine absorbed dose to water or air kerma are published in the book of code of practice by IAEA “Absorbed dose determination in external beam radiotherapy”: An international code of practice for dosimetry based on standards of absorbed dose to water” (Andreo, et al., 2006). The graphite wall makes the chamber almost water equivalent, the aluminium central electrode improves the energy response at energies below Co-60. The chamber is intended for the use in solid state phantoms and therefore not waterproof. The schematic diagram of cylindrical farmer chamber is shown in Figure 7.

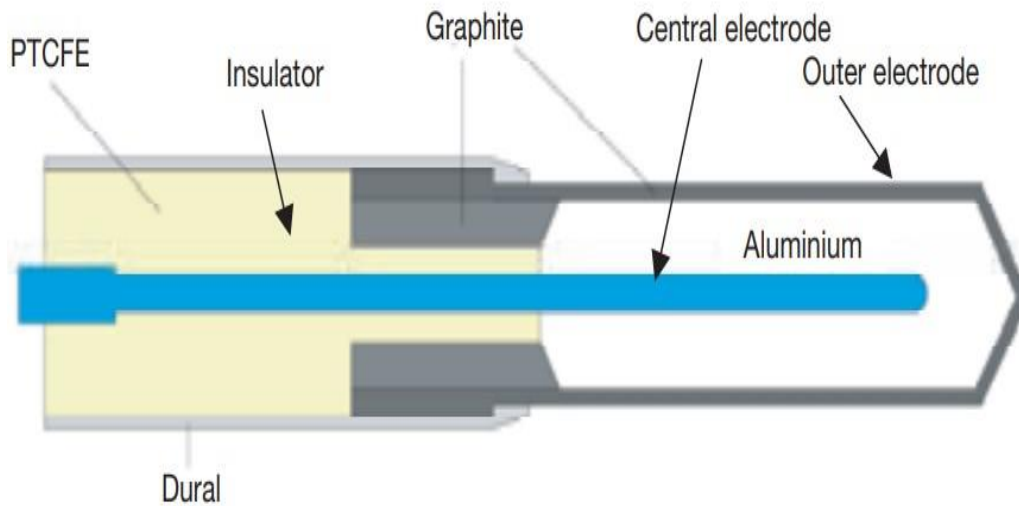


Figure 7: Basic design of a cylindrical farmer type ionization chamber (*Joanna & Govinda, 2005*).

2.7 Spherical ionization chamber

A spherical chamber consists of two concentric balls representing the central measuring electrode and the chamber wall and confining the sensitive volume. A guard on central electrode potential around the measuring electrode stem limits the dark current. The detector model type 32002 is designed for the measurement of ionizing radiation in radiation protection. It has a sensitive volume of 1 litre suitable for survey meter calibration and low-level measurements. The inside chamber diameter is 140 mm. The measuring quantity is air kerma and photon equivalent dose. It is used in conjunction with the electrometer at 400 voltage (V) nominal. Thus, it fulfils the requirement for excellent reproducibility and long-term stability of the sensitive volume. Superior features make the chamber suitable as standard chamber for calibration purposes. The spherical construction ensures a nearly uniform response to radiation from every direction. The energy response is very flat. This is achieved by the thin layer of aluminium on the inner wall surface, which provides for an increased photoelectric yield to compensate for the absorption of soft X-rays. The ranges which the spherical ionization chamber operate are as indicated in Figure 8.

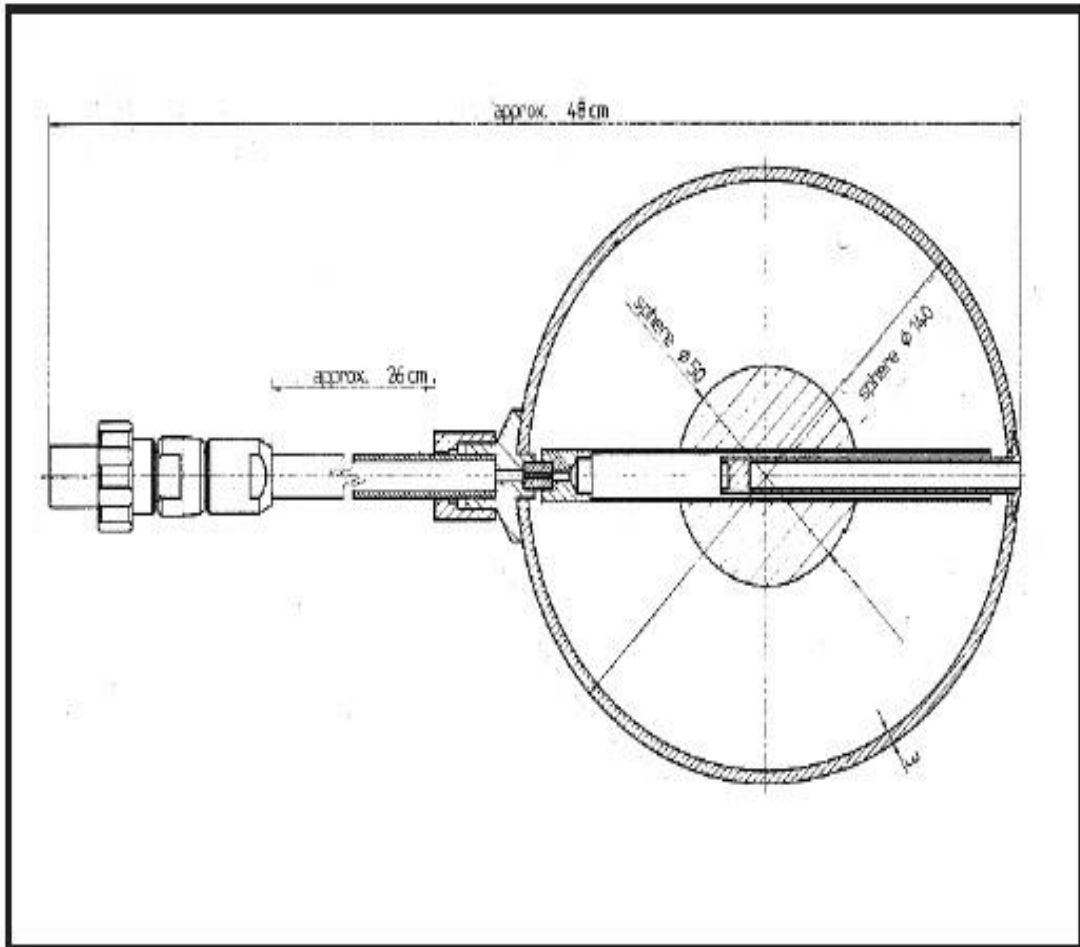


Figure 8: Litre spherical ionization chamber (*Joanna & Govinda, 2005*).

3 CHAPTER 3: MATERIALS AND METHODS

3.1 Introduction

The materials and the methods that were used in this study were based on the procedures that were developed in the Dosimetry Standards Laboratory (DSL) of the National Metrology Institute of South Africa (NMISA) in Pretoria. Two reference radiation detectors were used to obtain reference measurements in this study to characterize radio-photoluminescence glass dosimeters. Namely, the Physikalisch-Technische Werkstätten GmbH (PTW) spherical ionization chamber 1000 cc and the PTW cylindrical ionization chamber 0.6 cc. The two ionization chambers were used as the reference detectors to determine air kerma rate (i.e. dose rate) from three radiation sources (i.e. ^{60}Co , ^{137}Cs and ^{241}Am sources) located inside irradiators. In order to make a meaningful information of the radiation counts acquired by the glass dosimeters when exposed to radiation, the calibration coefficient of the glass dosimeter per each radiation source and correction factors were applied on the radiation counts.

Prior the irradiation of the glass dosimeters, the dose rate on the day of measurements was calculated from the calibration coefficients of the two ionization chambers and the charge measurements acquired. The charge measurements were acquired from ionization of air molecules inside the volume of mass of ionization chamber due to radiation. Ionization chambers were connected to the PTW electrometer for charge measurement readings. Irradiation times of the glass dosimeters were calculated from the dose rates and the prescribed doses of the glass dosimeters. Environmental conditions (temperature and pressure) were monitored during the duration of the measurements.

3.1 Environmental condition monitoring

3.1.1 Temperature and pressure

The detectors which are used in this study, particularly ionization chambers are corrected for temperature and pressure with humidity being monitored to allowable working conditions of the laboratory (SANAS, 2014). Temperature and pressure measurements were recorded before irradiation measurements (T_1 and P_1 for pre-irradiation) and after irradiation measurements (T_2 and P_2 for post-irradiation).

$$T(^{\circ}C) = \frac{T_1 + T_2}{2} - T_{corr} \quad (4)$$

$$P(mbar) = \frac{P_1 + P_2}{2} - P_{corr} \quad (5)$$

Where T_{corr} and P_{corr} are the temperature and pressure corrections between the reference measurement and the instrument's readings which were obtained during calibration measurements. Their values are obtained from the calibration certificates of the environmental monitors used (i.e. temperature and pressure monitors). Equation 4 and 5 are used to obtain interpolated temperature and pressure values which is found between two instrument's readings indicated on the calibration certificate.

Correction factor for temperature and pressure were calculated using equation 6:

$$K_{T,P} = \frac{1013.25}{P} * \frac{T + 273.15}{20 + 273.15} \quad (6)$$

3.2 Charge measurements

3.2.1 Background charge for pre (Q_{pre}) and post (Q_{post}) irradiation

Charge background measurements were recorded to quantify chamber leakages when the radiation source was off (i.e. pre and post-irradiation measurements) and the main measurements with the radiation source on (i.e. irradiation measurements). Background measurements were recorded for pre-irradiation and for post-irradiation to correct for any leakages which the ionization chambers might have experienced or picked up before and after irradiation measurements. The averages of the pre-irradiation (Q_{pre}) and post-irradiation (Q_{post}) were calculated using equation 7 and 8 and used to obtain corrected leakage measurements using equation 9 and finally the average of irradiation measurements was obtained by using equation 10.

$$Q_{pre}(C) = \frac{1}{n} \sum_{i=1}^n x_i \quad (7)$$

$$Q_{post}(C) = \frac{1}{n} \sum_{i=1}^n x_i \quad (8)$$

$$Q_{leakage}(C) = \frac{Q_{pre} + Q_{post}}{2} \quad (9)$$

$$Q_{Irr}(C) = \frac{1}{n} \sum_{i=1}^n x_i \quad (10)$$

Where:

Q_{pre} → average of the pre-irradiation measurements.

Q_{post} → average of the post-irradiation measurements.

$Q_{leakage}$ → average of pre (Q_{pre}) and post (Q_{post}) irradiation measurements.

Q_{Irr} → average of the irradiation measurements.

n → the total number of charge measurements.

x_i → the individual charge measurement.

3.2.2 Corrected charge collected during irradiation

Ten measurements were recorded for irradiation measurements, and their average was used to calculate corrected charge (Q) measurements as shown by equation 11:

$$Q(C) = Q_{Irr} - Q_{leakage} * K_{T,P} * K_{elec} \quad (11)$$

Where K_{elec} is the correction factor for the electrometer that was used to read charge measurements.

Table 3 displays electrometer factors used in this study.

Table 3: Electrometer factor.

Manufacture of electrometer	Electrometer Model	K_{elec}
PTW	T10009	1.004
PTW	10002	1.000

Electrometer - T10009 was used in ^{60}Co source measurements and 10002 was used in both ^{137}Cs and ^{241}Am source measurements as shown in Table 3.

3.3 Chamber calibration coefficients

Table 4: Calibration coefficients.

Manufacturer of ionization Chamber	Ionization chamber model	Radiation Sources	Calibration coefficient (Gy/C)
PTW	TW30010	^{60}Co	5.352E+07
PTW	TW32002	^{137}Cs	2.518E+04
PTW	TW32002	^{241}Am	2.513E+04

To ensure that the measurements are correct and acceptable in the metrology field, the chain of traceability is followed. The Primary Standards Laboratory (PSL) disseminate traceability measurement to the Secondary Standards Laboratory (SSD) and the SSD provide traceability to the industry or end-user. Thus, this chain is through calibration of the ionization chambers, and the calibration coefficient is the quantity that is used for traceability. Thus, the calibration coefficient converts the charge measurements collected from the ionization chamber to absorbed dose, it has the unit of Gy/C. A calibrated ionization chamber that was used in this study was obtained from the PSL

in United Kingdom; National Laboratory Standard (NPL). The cylindrical ionization farmer chamber was used as a reference chamber in the ^{60}Co source measurements and spherical ionization chamber was used as the reference chamber in both ^{137}Cs and ^{241}Am source. Calibration coefficient is denoted as N_k for air kerma measurements and $N_{D,W}$ for absorbed dose to water measurements as shown in Table 4.

3.4 Dose rate equation

$$\bar{D} = \frac{Q * N_k}{T} \quad (12)$$

$$\bar{D} = \frac{Q * N_{D,W}}{T} \quad (13)$$

Where T is the time taken for measurement collections. The dose rate (i.e. air kerma rate or absorbed dose rate to water) is calculated by equation 12 or 13 depending on the method used for measurements collection. Equation 12 is used if the measurements were taken in air and equation 13 if the measurements were taken with a solid water phantom.

3.5 Irradiation time

$$T = \frac{D}{\bar{D}} \quad (14)$$

Where D stands for absorbed dose. Irradiation time for Cs-137 and Am-241 was in the units of seconds and Co-60 in the units of minutes as entered in the irradiation software of each radiation source. The effect of intrinsic that was tested using ionization chambers, through the effect that it has when the source is moving from safe position to the irradiation position (when the source is opened for exposure) and when the source is moving back to the safe position (when source is stopped for exposure). No signal was detected during intrinsic time measurements by the ionization chambers. Ionization chambers are more sensitive to low radiation than glass dosimeters and yet the contribution of intrinsic time was not detected using them. It was then concluded that intrinsic time had no effect on the irradiation measurements on reference detectors and RPLGDs.

3.6 Cylindrical ionization farmer chamber used in Co-60 source measurements

The farmer chamber was maintained monthly by taking beam outputs measurements on a ^{60}Co source at the distance of 100 cm from the source to the centre of the chamber. The dose rate measured was compared with the average of previous dose rate measurements, and it was found to be within acceptable percentage (i.e. 1.0 %). Thus, this is a procedural requirement of the laboratory to ensure that the chamber is not out of calibration, and the readings are consistent and reproducible. The calibration coefficient ($N_{D,W}$) for ^{60}Co source was obtained from the calibration certificate of the chamber, calibrated in water at the Primary Standards Laboratory (PSL) at BIPM in France. Thus, $N_{D,W}$ was given as $5.32\text{E}+07$ Gy/C. The farmer chamber has a volume of 0.6 cm^3 (or 1 litre) and the diameter of 6.1 mm (inner diameter).

3.7 Co-60 radiation source

The ^{60}Co nucleus when it decays, it releases one electron with 317.9 keV energy and two gamma quanta with energies of 1.173 MeV and 1.332 MeV. The collimator of ^{60}Co source, has the diameter that is adjustable to the desired field size particularly to 10 cm x 10 cm at the reference distance of 100 cm from the centre of the source position. The source has an activity of 329.3 TBq (8 900 Ci).

3.8 Set-up in the Co-60 source

3.8.1 Set-up of cylindrical ionization farmer chamber in Co-60 beam

The two laser beams which are mounted on the walls perpendicular to each other, were used to set-up the farmer chamber in the ^{60}Co source. One laser beam was fixed horizontally along the beam axis (used as a reference position along the centre of the beam axis) and the other one was fixed at 100 cm (used as a reference beam when setting up the detector) from the source as shown in Figure 9. The two laser beams were crossing at the centre of the ionization chamber, and this implied that the centre of the chamber was positioned exactly at 100 cm from the source.

The chamber was inserted inside a solid water phantom of 30 cm x 30 cm x 15 cm depth. The solid water phantom had marking that indicated the centre of the chamber were the two lines (i.e. horizontal and vertical) were crossing. Thus, the phantom was introduced as a medium on the Co-60 source to create the scatter effect during ionization of air molecules inside the volume of the chamber.

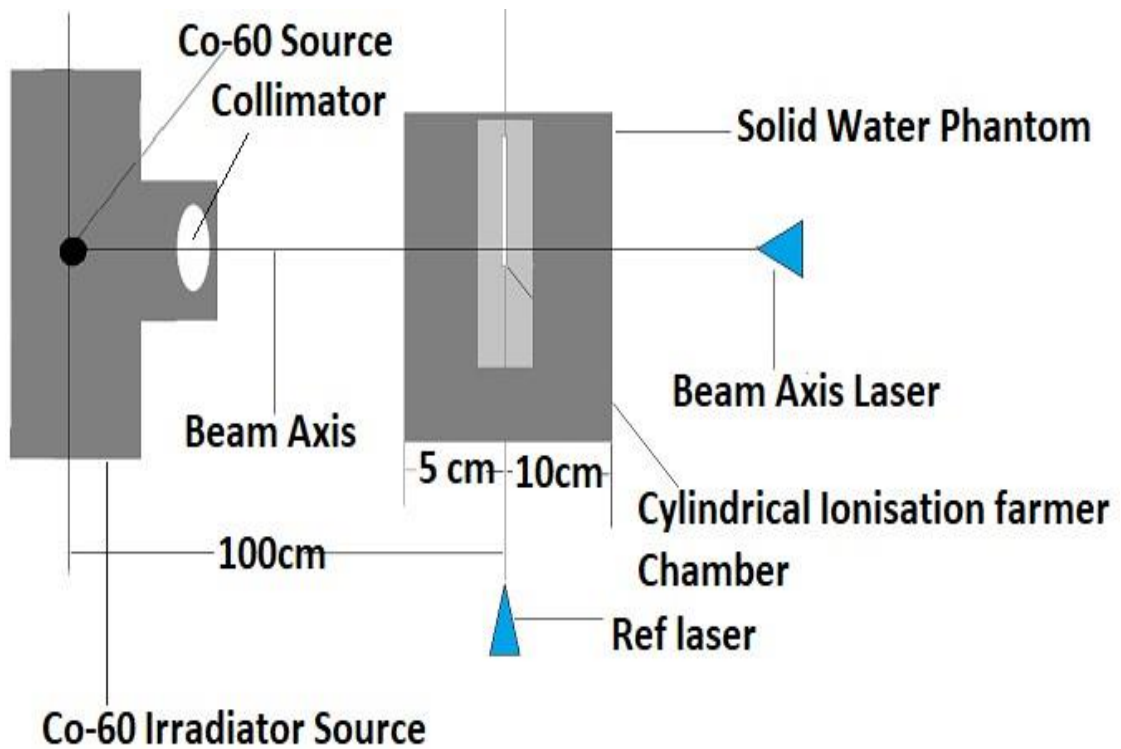


Figure 9: Ionization farmer chamber set-up in the Co-60 source.

3.8.2 Set-up of RPLGD in Co-60 beam

The substitution method was used to replace the farmer chamber with RPL glass dosimeters and nothing else was changed on the set-up depicted in Figure 9 to 10. The holder of the glass dosimeters had five slots, only three were used (three middle slots) to irradiate the glass dosimeters. The first and the fifth slots were left vacant during irradiations. The two laser beams were passing in the centre of the middle glass dosimeter as it was with the farmer chamber. Fifty-eight (58) glass dosimeters were irradiated with the ^{60}Co source for the duration of time calculated from the dose rate of the chamber and prescribed dose.

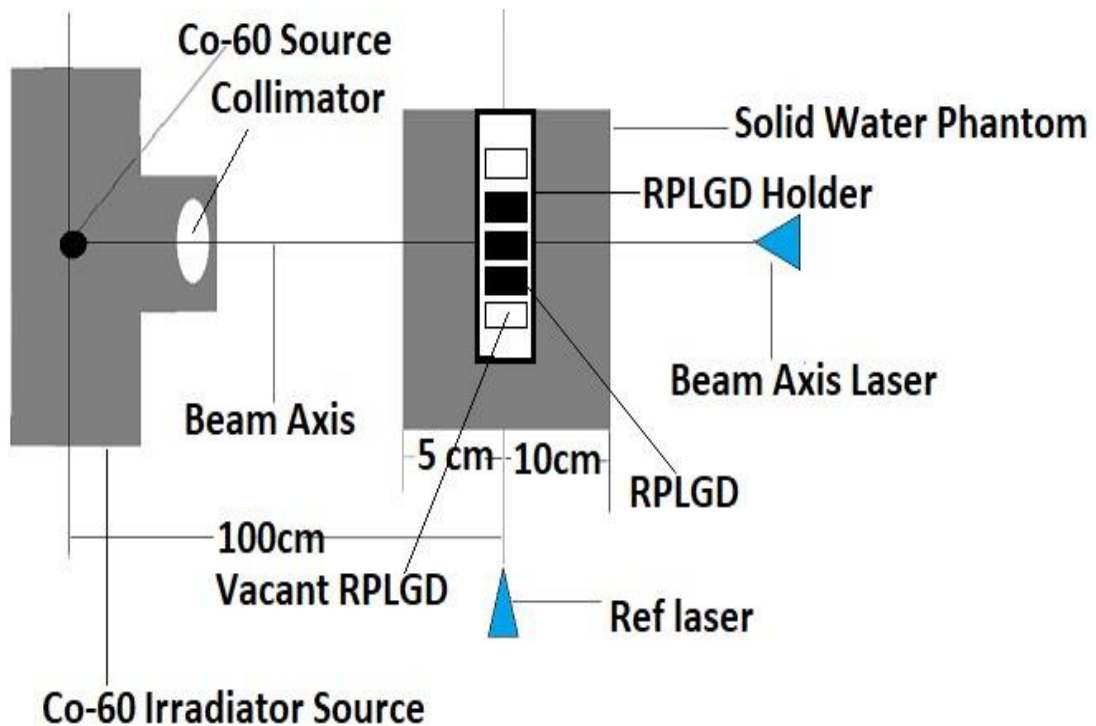


Figure 10: RPLGD set-up in the Co-60 source.

3.9 Spherical ionization chamber used in Cs-137 source measurements

The spherical ionization chamber is maintained on monthly basis through beam outputs measurements on ^{137}Cs and ^{241}Am sources at the distance of 200 cm from the source from the centre of the source. The calculated dose rate was compared with the previous month dose rate measurements, and it was found to be of acceptable percentage (1.0 %). Also, this is a procedural requirement of the laboratory to ensure that the ionization chamber is not damaged, and the readings are consistent and reproducible. The calibration coefficient (N_k) for ^{137}Am source was given as $2.518\text{E}+04$ Gy/C from its calibration certificate. The chamber has a volume of 1000 cm^3 and the diameter of 140 mm.

3.10 Cs-137 radiation source

The ^{137}Cs source and is primarily used for traceability through calibrations of radiation protection instruments such as; radiation ionization chambers, survey meters, TLDs and etc. The source has an

energy of 661 keV and the activity of 2.22 TBq. Similarly, with the Co-60 source, two lasers were used in the ^{137}Cs source set-up for the beam axis and for ref laser beam.

3.10.1 Set-up in the Cs-137 source

3.10.2 Set-up of spherical ionization farmer chamber in Cs-137 beam

Similarly, to ^{60}Co source, the two laser beams which are mounted on the walls perpendicular to each other, were used to set-up the spherical chamber in the ^{137}Cs beam. One laser beam was fixed horizontally along the beam axis (used as a reference position along the centre of the beam axis) and the other one was fixed at 200 cm (used as a reference laser beam when setting up the detector) from the source as shown in Figure 11. The two laser beams were crossing at the centre (i.e. at 200 cm from the centre of the source) of the chamber.

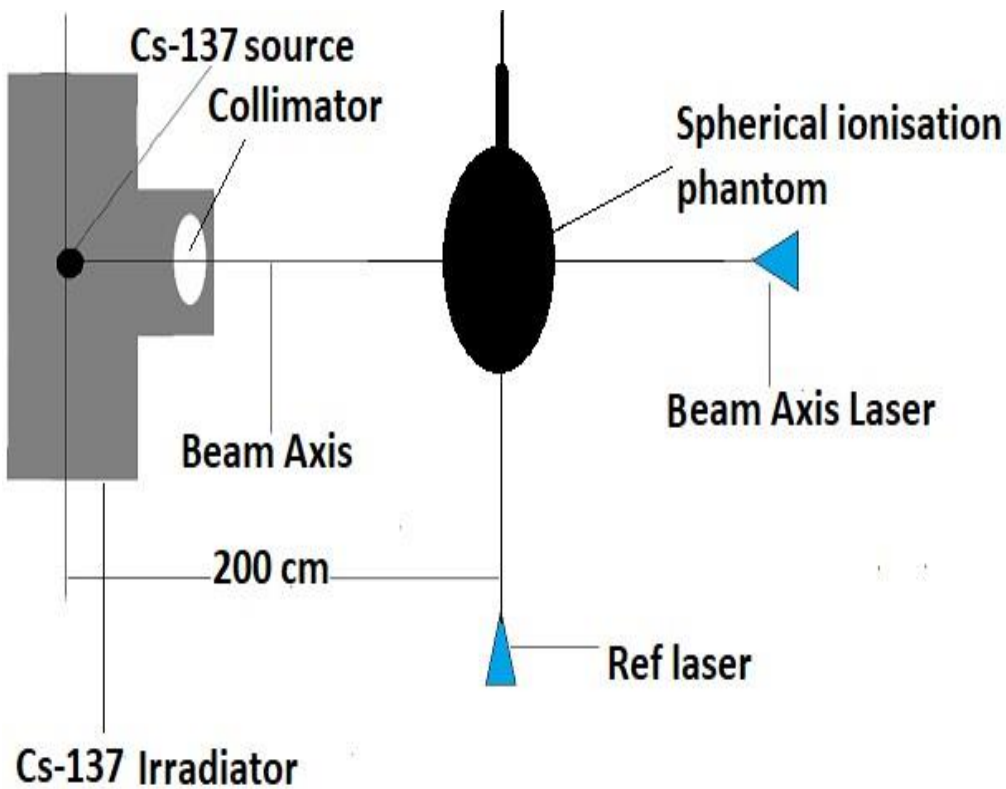


Figure 11: Spherical ionization chamber set-up in ^{137}Cs source.

3.10.3 Set-up of RPLGD in Cs-137 beam

The substitution method was also used to replace the spherical ionization chamber with glass dosimeters as shown in Figure 12. Five glass dosimeters were positioned at a time for irradiation. Two laser beams were passing in the centre of the glass dosimeters similarly as it was in the case of the ionization chamber setup. Thirty-five (35) glass dosimeters were irradiated with ^{137}Cs source.

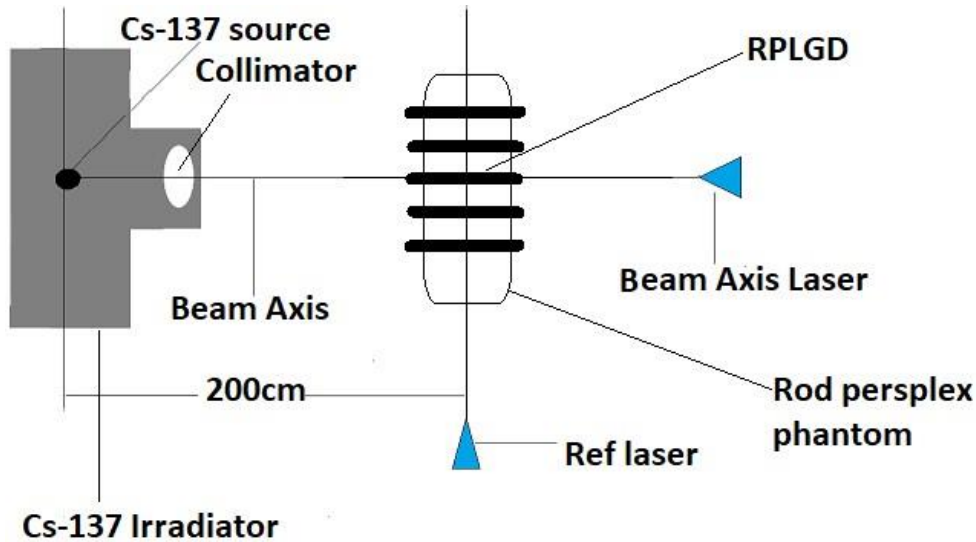


Figure 12: RPLGD set-up in the ^{137}Cs source.

3.11 Spherical ionization chamber used in Am-241 source measurements

The spherical ionization chamber used in ^{241}Am source measurements, is the same one that was used in the ^{137}Cs source measurements. Thus, the same maintenance is also done for ^{241}Am source on monthly basis. However, the measurements were carried out on the different irradiator than the one used on other sources. The dose rate measured was compared with the average of previous dose rate measurements, and it was found to be within acceptable percentage (i.e. 1.0 %). The calibration coefficient (N_k) for ^{241}Am source is given as $2.513\text{E}+04$ Gy/C.

3.12 Am-241 radiation source

The ^{241}Am source emits alpha radiation with traces of gamma radiation being observed. The source has activity of 37 GBq and the energy of 59.5 keV.

3.13 Set-up in the Am-241 source

3.13.1 Set-up of spherical ionization chamber in Am-241 beam

The set-up of the spherical ionization chamber in the ^{241}Am source is similar to the other two sources whereby the substitution method was used as shown in Figure 13. However, the centre of the ionization chamber was positioned at 50 cm from the source. Am-241 source has a low activity hence the distance of the detector to the source is too small for the detector to be able to measure some significant amount of radiation level.

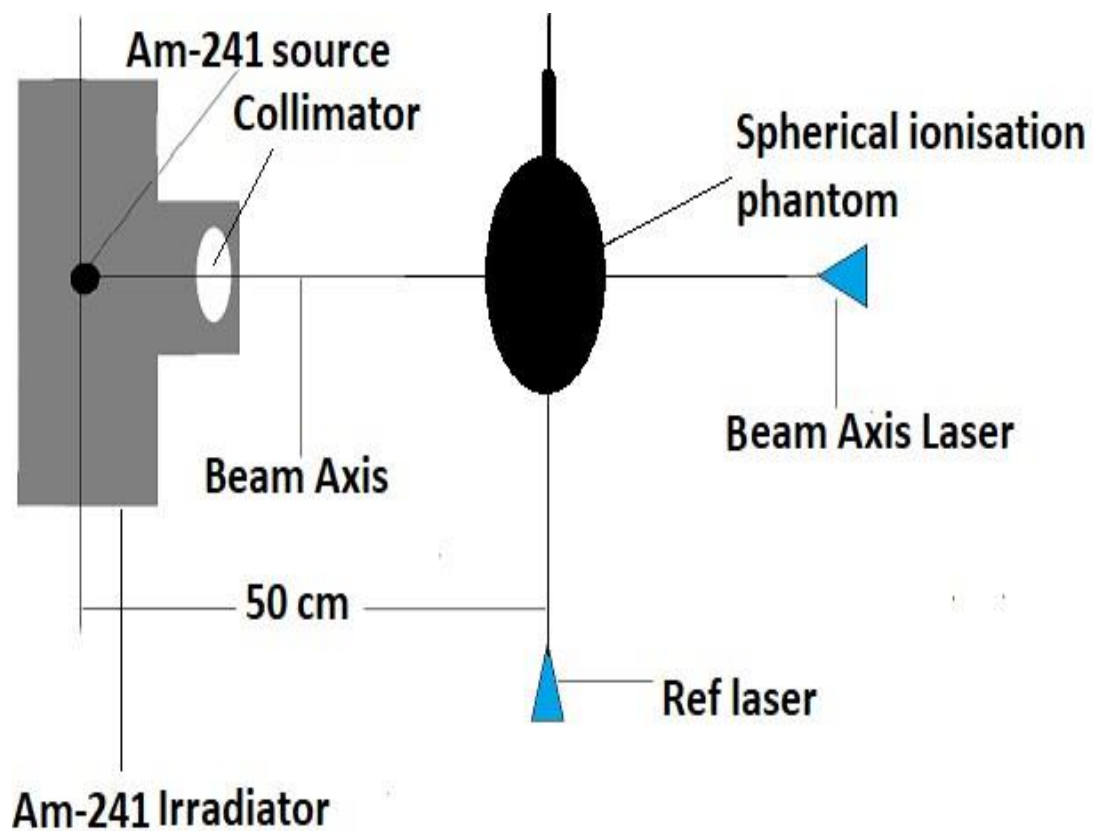


Figure 13: Spherical ionization chamber set-up in ^{241}Am source.

3.13.2 Set-up of RPLGD in Am-241 beam

Twenty-one (21) glass dosimeters were irradiated with ^{241}Am source. Three were set to be irradiated at once in the plastic perspex that was used in the irradiation of the glass dosimeter in ^{137}Cs source. The time that was taken to irradiate the glass dosimeters in Am-241 source was long due to strength

of the source, hence only few glass dosimeters could be irradiated with low prescribed doses for feasible time for measurements collection. Figure 14 shows the set-up of glass dosimeters in the ^{241}Am source.

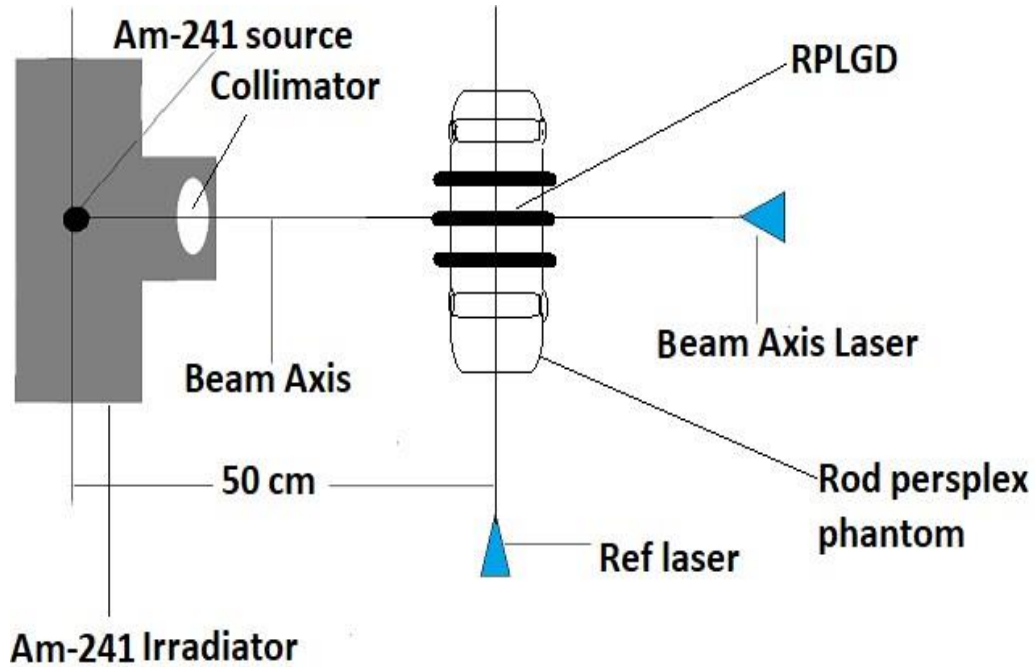


Figure 14: RPLGD set-up in ^{241}Am source.

3.14 Prescribed doses used to irradiate RPLGD

Table 5: Prescribed doses for the three sources.

Sources	1	2	3	4	5	6	7	8	9	10	Units
Co-60	200	500	800	1000	1500	2000	300	5000	7000	9000	mGy
Cs-137	10	15	20	25	30	35	40				mGy
Am-241	20	40	60	80	100	120	140				μGy

Prescribed doses are the absorbed dose that was expected to be read on the glass dosimeters after irradiations. of the glass dosimeters with respective radiation sources. Each source has the reference

doses that were used to calculate calibration coefficient of the glass dosimeter. The reference doses are as indicated by bold numbers in Table 5 for the sources.

3.15 Glass element

Radio-photoluminescence glass dosimetry system that was used in this study was manufactured by AGC TECHNO GLASS CO., LTD. The model number for the glass dosimeters used is RPL glass element for IAEA (type FD-R1.5(12)-7). A Total of 58 radio-photoluminescence glass dosimeters were used in this study. Each glass element has the diameter of 1.5 mm and 12 mm length. The glass dosimeter and its plastic holder have unique ID marking. Before the glass dosimeters were used, they were cleaned with ethanol to remove any dust or contaminations. The glass dosimeters were inserted in their special plastic holder with the ID making facing upright as shown in Figure 15.

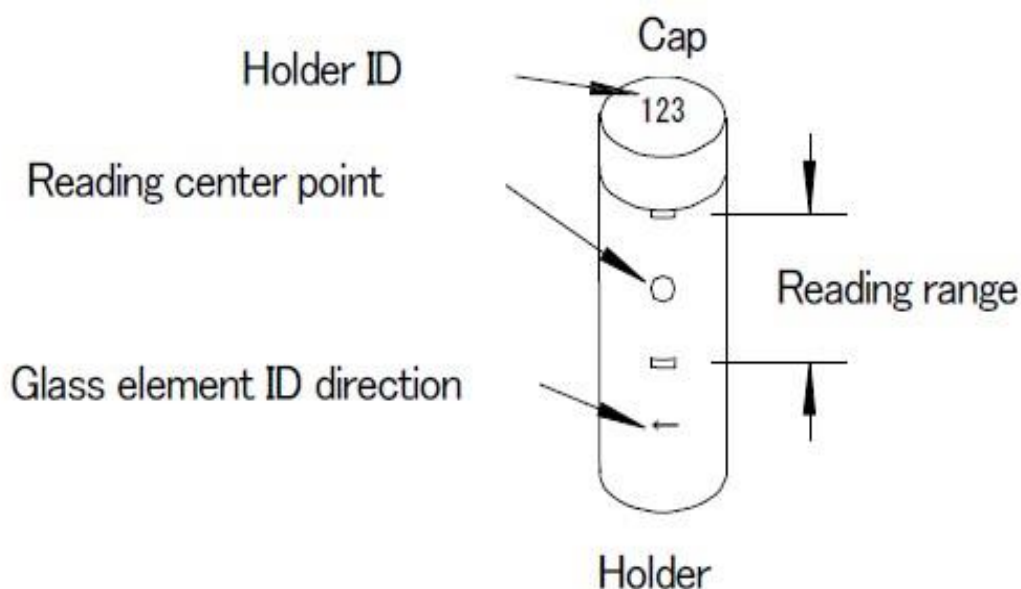


Figure 15: Reading centre point and reading range of glass dosimeter (*LTD AGC TECHNO GLASS CO, 2008*).

3.16 Loading the RPLDs using a tweezer or loading device

The loading device and tweezer are simple devices manufactured by AGC TECHNO GLASS CO., LTD to insert the glass elements inside the holder and or removing them. The tweezer is also used to grab the glass element into the read-out magazine or to the holder, and the loading device was used

to transfer glass dosimeters to magazine or back to the holder. Figure 16 shows the pictures of a tweezer and loading device.

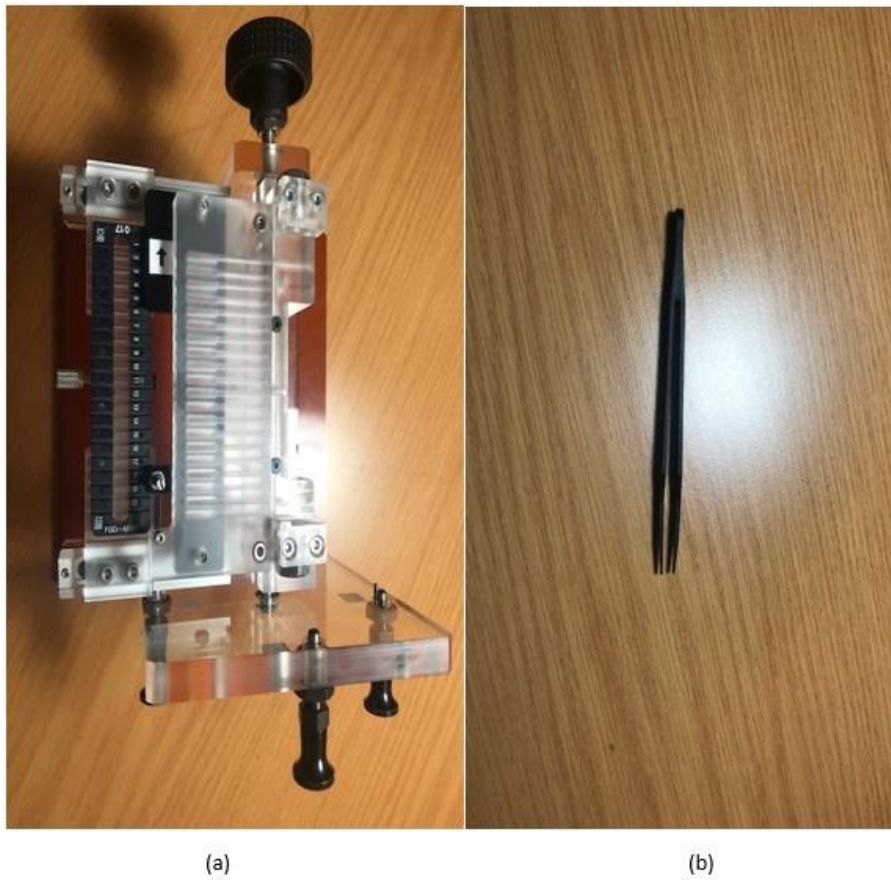


Figure 16: (a) loading device and (b) tweezer.

3.17 Annealing magazine and read-out magazine

The read-out magazine is made out of plastic material that can stand the temperature of 70 °C. It is used when the radiation signal of the glass dosimeter is read using Dose Ace Reader or to transfer the glass dosimeters in or out of the dosimeter holder when using loading device shown in Figure 16 (b). Annealing magazine is used to anneal the glass dosimeters at the temperature of 400 °C. The two magazines have maximum slots to position 20 glass dosimeters and with the ID indication of how they should be positioned, and in addition the read-out magazine has written numbers from 1 to 20. The two magazines are shown in Figure 17.

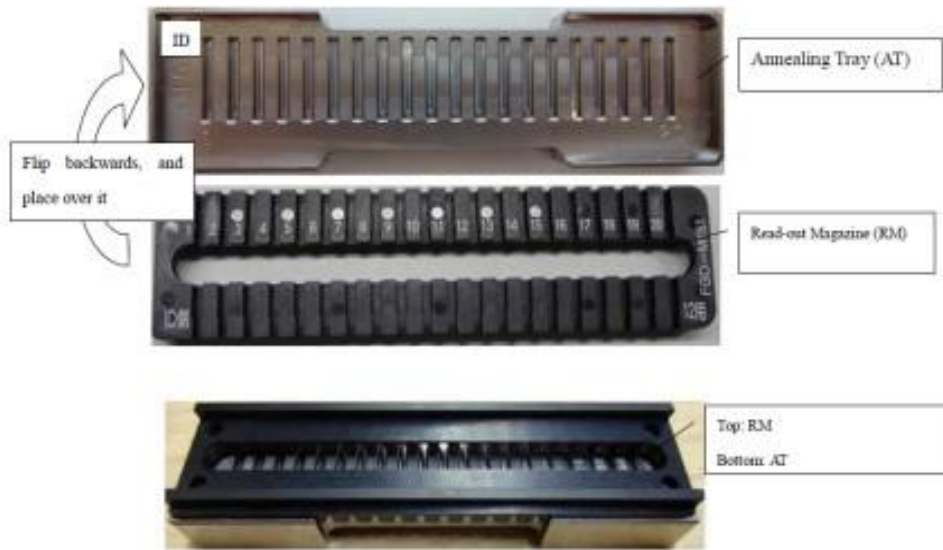


Figure 17: Magazine reader and annealing magazine.

3.18 Annealing and pre-heat oven

When the glass dosimeters were pre heated, program one (1) was selected on the oven shown in Figure 18 and the two arrows facing opposite directions were pressed at the same time to run the program. Similarly, when the glass dosimeters are annealed, program two (2) is selected and the two arrows are pressed simultaneously to run the program. The glass dosimeters were annealed before they were irradiated at the temperature of 400 °C and allowed to cool for at least two hours. When the glass dosimeters are heated at the temperature of 400 °C, the electrons return to the valence band. The background counts that were recorded after annealing were subtracted from the absorbed radiation counts. After irradiations of the glass dosimeters, before reading them, they were pre heated at temperature of 70 °C in the oven to excite the captured electrons to the conduction band for at least an hour then cleaned with ethanol in the ultrasonic bath to remove any contamination.



Figure 18: Annealing and pre-heating oven.

3.19 Dose Ace reader (FGD-1000)

The Dose Ace reader is used to read the glass dosimeter in the magazine reader, depicted in Figure 19. The reader is able to read from lower dose of 0.01 mGy or (mSv) to higher dose 10 Gy or (Sv). It can further read to high dose option application to maximum of 100 Gy or (Sv). Thus, the reader is only set to measure from lower dose application and is used in this mode only in this study. A maximum of 20 glass dosimeters can be read on one session and accumulated radiation signal is displayed on the controller screen. Results were saved as excel data file. Figure 19 shows Dose Ace FGD-1000 and computer connected to the reader for which has the software to read radiation counts from the glass dosimeter. The reader uses pulse UV laser for excitation of electrons. When excited by pulse UV laser, the silver phosphate glass emits 600 to 700 nm visible orange light and return to original colour centre. The counts acquired from the glass dosimeter is linearly proportional to the amount of radiation absorbed, this is achieved by applying all the corrections on the radiation counts to convert it to the absorbed dose accumulated by the glass dosimeters.



Figure 19: Dose ace reader FGD-1000.

3.20 Magazine correction factors

Magazine numbered 018 was used as a read-out magazine. Read-out magazine has twenty (20) positions which the RPL glass dosimeters are inserted on for reading. Twenty RPLGD were irradiated with 2 Gy in the Co-60 beam, each was read on all 20 positions. The global average of all the readings was calculated, and each reading was normalized to the global average. It was discovered during that when one glass dosimeter was read in all 20 slots of magazine, the readings were not the same depending where the glass dosimeter is positioned on the magazine. Thus, this influence of magazine corrections was corrected by determining magazine correction for every position. The magazine correction factors (f_{mag}) were determined for position dependence. The radiation counts for glass dosimeters were then corrected for all the position to remove the influence of the positions for all the radiation source measurements. Magazine corrections for each position was fitted on second degree polynomial for determining the function used for calculating magazine corrections factors.

3.21 Sensitivity correction factors for glass dosimeters

The difference in each glass dosimeter's mass or response to radiation is corrected by the factor called the sensitivity correction factor. This factor is corrected on the glass dosimeters that are exposed to the same radiation dose. The glass dosimeters are irradiated in groups, and the sensitivity correction

factor for each glass dosimeter is determined through the average dose for each group. The sensitivity correction factor for each glass dosimeter was determined using equation 15.

$$f_{SCF} = \frac{M_i}{\bar{M}_i} \quad (15)$$

Where M_i is the individual glass signal and \bar{M}_i is the average of all glass dosimeter signal. The sensitivity correction factors were used to correct for each individual glass dosimeter signal during the measurements.

3.22 Non-linearity and linearity correction factors

To test the non-linearity effect of the absorbed dose on glass dosimeters and to determine the linearity correction factors, a total of 58 dosimeters were used in this study. In the Co-60 measurements, nine groups of dosimeters consisted of 6 individual glass dosimeters and one group had four glass dosimeters. A total of ten groups were irradiated in Co-60 measurements. The glass dosimeters were irradiated using different doses from 200 to 9000 mGy. In the Cs-137 measurements, seven groups which consisted of five individual glass dosimeters per group were irradiated with different doses from 10 to 40 mGy. Lastly, in the Am-241 measurements, seven groups which consisted of three individual glass dosimeters per group were irradiated with different doses from 20 to 140 μ Gy as indicated in Table 12. The glass dosimeters were read with magazine 018. Magazine correction factors and sensitivity correction factors were applied to the measured radiation counts. The corrected counts were normalized to the radiation counts at 2 Gy to determine the non-linearity correction factors. Thus, linearity correction factors were calculated as the inverse of the non-linearity correction factors using equation 16.

$$f_{lin} = \frac{1}{f_{non-lin}} \quad (16)$$

Where $f_{non-lin}$ is the non-linearity correction factor.

3.23 Calibration coefficient of RPLGD in Co-60 beam

The two ionisation chambers that were used in this study as the reference detectors have their own calibration coefficients. Cylindrical ionization farmer chamber which was used as the reference chamber in ^{60}Co measurements has the absorbed dose to water calibration coefficient $N_{RPLGD}(^{60}\text{Co})$. The calibration coefficient for the farmer chamber was obtained from its calibration certificate of measurements. Similarly, the calibration coefficient for glass dosimeter was determined for absorbed dose to water with the solid water measurements taken with the glass dosimeter inside the solid water phantom. The radiation counts obtained when the glass dosimeters were irradiated with prescribed radiation dose of 2 000 mGy were taken to be the reference radiation dose ($M_{ref,2000mGy}$). Equation 17 was used to calculate calibration coefficient $N_{RPLGD}(^{60}\text{Co})$.

$$N_{RPLGD}(Co60) = \frac{M_{ref,2000mGy}}{\bar{M}_{2000mGy}} \quad (17)$$

Where $\bar{M}_{2000mGy}$ is the average of all radiation counts irradiated with prescribed dose of 2 000 mGy (i.e average radiation counts of the six glass dosimeters exposed to reference dose). The reference dose was taken at 100 cm from the centre of the radiation source to the centre of the middle glass dosimeter of each three-glass dosimeter position as a set on the beam axis.

3.24 Air kerma calibration coefficient of RPLGD in Cs-137 beam

The spherical ionization chamber was used as the reference detector in the measurements of ^{137}Cs source in air. The Air kerma calibration coefficient ($N_{RPLGD}(^{137}\text{Cs})$) for the glass dosimeter with the rod perspex was calculated using equation 18. The radiation counts obtained when the glass dosimeter was irradiated with prescribed radiation dose of 20 mGy was taken to be the reference radiation dose ($M_{ref,20mGy}$).

$$N_{RPLGD}(Cs137) = \frac{M_{ref,20mGy}}{\bar{M}_{20mGy}} \quad (18)$$

Where \bar{M}_{20mGy} is the average of all radiation counts irradiated with prescribed dose of 20 mGy (i.e average radiation counts of the five glass dosimeters exposed to reference dose). The reference dose

was taken at 200 cm from the centre of the radiation source to the centre of the middle glass dosimeter of each three-glass dosimeter position as a set on the beam axis.

3.25 Air kerma calibration coefficient of RPLGD in Am-241 beam

The spherical ionisation chamber was also used as the reference detector in the measurements of ^{241}Am source in air. Air kerma calibration coefficient ($N_{RPLGD} (^{241}\text{Am})$) for the glass dosimeter with the rod perspex was calculated using equation 19. The radiation counts obtained when the glass dosimeters were irradiated with prescribed radiation dose of $20 \mu\text{Gy}$ was taken to be the reference radiation dose $M_{ref,20\mu\text{Gy}}$.

$$N_{RPLGD}(\text{Am241}) = \frac{M_{ref,20\mu\text{Gy}}}{\bar{M}_{20\mu\text{Gy}}} \quad (19)$$

Where $\bar{M}_{20\mu\text{Gy}}$ is the average of all radiation counts irradiated with prescribed dose of $20 \mu\text{Gy}$ (i.e average radiation counts of the three glass dosimeters exposed to reference dose). The reference dose was taken at 50 cm from the centre of the radiation source to the centre of the middle glass dosimeter of each three-glass dosimeter position as a set on the beam axis.

3.26 RPLGD absorbed dose

The amount of radiation exposed to the glass dosimeters is linearly proportional to the absorbed dose by glass dosimeters. To relate the radiation counts absorbed by the glass dosimeters to absorbed dose (D_{Abs}), equation 20 was used.

$$D_{Abs} = M * f_{mag} * f_{SCF} * f_{lin} * N_{RPLGD} \quad (20)$$

The difference of the absorbed dose on the glass dosimeter as oppose to the prescribed dose (D_{Pre}) is also being measured by the percentage difference which is calculated by equation 21.

$$\% \text{ Difference} = \frac{D_{Abs} - D_{Pre}}{D_{Pre}} * 100 \% \quad (21)$$

4 CHAPTER 4: RESULTS AND DISCUSSIONS

4.1 Introduction

RPL glass dosimeters were characterized against the reference detectors using the substitution method (i.e. exchange of ionization chambers with glass dosimeters under the same set-up conditions). Three radiation sources; ^{60}Co , ^{137}Cs and ^{241}Am , were used to measure gamma radiation response of the glass dosimeters with known radiation doses (prescribed doses (D_{Pre})). Correction factors were applied to the accumulated radiation counts on the glass dosimeter's response to remove all the influences or contributions which were not due to the irradiation of the glass dosimeters. A total of fifty-eight (58) glass dosimeters were used in this study. The signal acquired for each source was erased after been read multiple times to reuse the glass dosimeters for the other sources. Thus, this means that the same sets of dosimeters were irradiated with three sources. All 58 glass dosimeters were used in the measurements of ^{60}Co source, thirty-five (35) were used in ^{137}Cs source and twenty-one (21) were used in ^{241}Am source measurements. Magazine correction factors for position dependence correction for 20 slots are shown in Annexure 1, and individual results for the measurements to calculated absorbed dose of the glass dosimeters are shown in Annexure 2 to 4.

4.2 Magazine correction factors

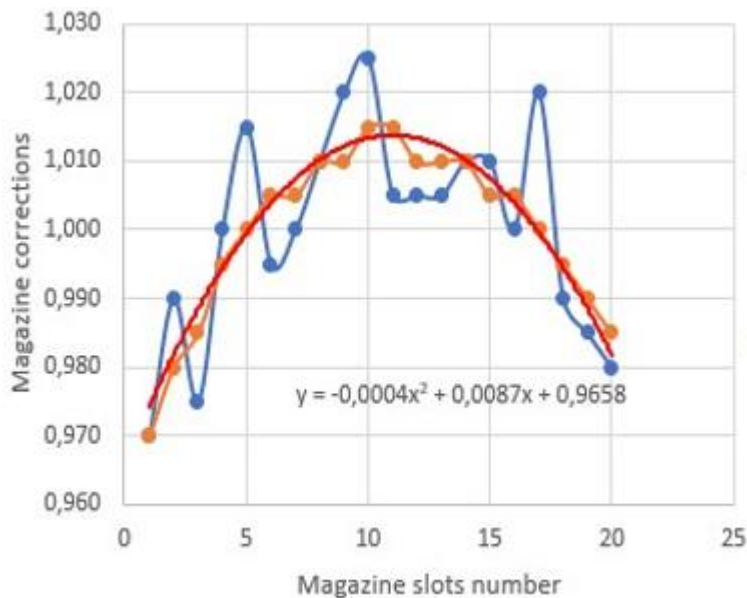


Figure 20: Magazine correction factors for actual data, correction factors and curve fitting.

Magazine 018 was used throughout the radiation counts measurement readings for all the sources. Figure 20 shows magazine correction factors plotted against 20 magazine position slots. A second order polynomial was also fitted for determining the function used for calculating magazine correction factors (red curve), actual data is represented by a blue curve and calculated correction factors are represented by an orange curve. Equation 22 was used to calculate a second order polynomial function.

$$f_{mag} = -0.0004P^2 + 0.0087P + 0.09658 \quad (22)$$

Where P is the magazine position slot.

Table 18 on Annexure 1 shows magazine correction factors for each 20 position slots for both actual data and curve fit rounded off within 0.005. Thus, magazine correction factors are used throughout the measurements for position correction of the magazine reader.

4.3 Environmental condition measurements

Temperature and pressure measurements were monitored and kept under control in the laboratory for the duration of measurements. Humidity was monitored during the measurements. The measurements were not corrected for humidity. Thus, temperature and pressure measurements were corrected as follows below.

4.3.1 Temperature and pressure measurements

Table 6 shows the environmental conditions for temperature and pressure measurements for ^{60}Co , ^{137}Cs and ^{241}Am sources. Relative humidity recorded for the source were as follows; 54.20 %rh, 42.40 %rh and 50.00 %rh.

Table 6: Temperature and pressure for radiation sources.

Source	Temperature (°C)				Pressure (mbar)			
	T_1	T_1	T_{corr}	T	P_1	P_1	P_{corr}	P

Co-60	18.380	18.383	0.005	18.377	874.44	874.32	-0.08	874.46
Cs-137	20.271	20.271	0.100	20.171	869.69	869.60	-0.020	869.67
Am-241	19.300	19.100	-0.200	19.400	868.23	868.47	-0.050	868.40

4.3.2 Correction factors for temperature and pressure

Table 7 shows correction factors for temperature and pressure measurements for three radiation source measurements. Relative humidity was monitored on the day of measurements.

Table 7: Correction factors for temperature and pressure for three sources.

Correction factor ($K_{T,P}$)	Co-60	Cs-137	Am-241
$K_{T,P}$	1.152297273	1.165783432	1.164412882

4.4 Charge measurements

4.4.1 Pre and post-irradiation charge measurements with cylindrical ionization farmer chamber in Co-60 beam

Background measurements for leakages for both pre and post-irradiations charge measurements with cylindrical ionization chamber in ^{60}Co source are shown in Table 8.

Table 8: Leakage measurements for Co-60 source.

	Pre-irradiations (C)	Post-irradiations (C)
1	8.00E-14	1.00E-14
2	6.00E-14	4.00E-14
3	9.00E-14	4.00E-14

4	8.00E-14	4.00E-14
5	9.00E-14	7.00E-14
6	1.00E-14	8.00E-14
Average Charge (Q)	6.83333E-14	4.66667E-14

Q_{Pre} and Q_{Post} in Table 6 were calculated using equation 7 and 8. The average charge measurements (i.e. leakage charge measurements) for pre and post-irradiation were calculated using equation 9.

$$Q_{leakage} = \frac{Q_{Pre} + Q_{Post}}{2} = \frac{6.83333E-14 + 4.66667E-14}{2} = 5.75E-14 \text{ C}$$

4.4.2 Pre and post-irradiation charge measurements with spherical ionization chamber in Cs-137 beam

Background measurements for leakages for both pre and post-irradiations charge measurements with spherical ionization chamber in ^{137}Cs source are shown in Table 9.

Table 9: Leakage measurements for Cs-137 source.

#	Pre-irradiations (C)	Post-irradiations (C)
1	3.00E-14	2.00E-14
2	-2.00E-14	-8.00E-14
3	-1.00E-14	-5.00E-14
4	-4.00E-14	-3.00E-14
5	-2.00E-14	-2.00E-14
Average Charge (Q)	-1.20000E-14	-3.20000E-14

Leakage charge measurements for Cs-137 source was calculated using equation 9:

$$Q_{leakage} = -2.20000E -14 C$$

4.4.3 Pre and post-irradiation charge measurements with spherical ionization chamber in Am-241 beam

Background measurements for leakages for both pre and post-irradiations charge measurements with spherical ionization chamber in ²⁴¹Am source are shown in Table 10.

Table 10: Leakage measurements for ²⁴¹Am source.

#	Pre-irradiations (C)	Post-irradiations (C)
1	2.00E-14	-1.10E-14
2	-7.00E-14	-2.10E-14
3	-6.00E-14	-3.10E-14
4	-6.00E-14	-4.40E-14
5	-8.00E-14	-4.30E-14
6	-2.00E-14	-3.50E-14
Average Charge (Q)	-7.83333E-14	-3.08333E-14

Equation 9 was used to calculate leakage charge (i.e. $Q_{leakage}$).

$$Q_{leakage} = -1.93333E-13 C$$

4.4.4 Irradiation charge measurements in Co-60, Cs-137 and Am-241 source

Ten irradiation charge measurements were taken for each source with the source on, and the measurements are shown in Table 11.

Table 11: Irradiation charge measurements for Co-60, Cs-137 and Am-241 source.

#	Co-60 charge readings (C)	Cs-137 charge readings (C)	Am-241 charge readings (C)
1	-7.246E-09	-8.979E-09	-1.320E-10
2	-7.246E-09	-8.979E-09	-1.320E-10
3	-7.247E-09	-8.980E-09	-1.320E-10
4	-7.248E-09	-8.978E-09	-1.315E-10
5	-7.247E-09	-8.978E-09	-1.320E-10
6	-7.248E-09	-8.979E-09	-1.320E-10
7	-7.248E-09	-8.980E-09	-1.315E-10
8	-7.248E-09	-8.977E-09	-1.315E-10
9	-7.248E-09	-8.974E-09	-1.315E-10
10	-7.248E-09	-8.978E-09	-1.315E-10
Average charge (Q_{Irr})	-7.24740E-09	-8.97820E-09	-1.31750E-10

Average charge (Q_{Irr}) for Co-60, Cs-137 and Am-241 source collected during irradiations is shown in Table 9 calculated using equation 10.

4.4.5 Corrected charge measurements for Co-60, Cs-137 and Am-241 source

Equation 11 was used to calculate the corrected charge (Q) inside the volume of ionization chamber which was caused by interaction of radiation with air molecules. Table 12 displays corrected charge measurements for ^{60}Co , ^{137}Cs and ^{241}Am source.

Table 12: Charge measurements.

Source	Co-60	Cs-137	Am-241
Q (C)	$-8.38463E-09$	$-1.04666E-09$	$-1.53186E-10$

4.5 Dose rate results

Charge measurements for ^{60}Co and ^{137}Cs sources were taken at the interval of 30 seconds, and ^{241}Am source at 60 seconds interval. The values of the calibration coefficients are listed in Table 4. The dose rates for the three sources were calculated using equation 12 or 13. Irradiation time for ^{60}Co source set on the irradiator unit was in minutes with a resolution of two decimal numbers. The two irradiator units for ^{137}Cs and ^{241}Am source were using seconds for setting irradiation times, however ^{137}Cs irradiator unit had a resolution of one decimal number and for ^{241}Am source it had zero resolution decimal number.

4.5.1 Co-60 source dose rate

Equation 12 was used to calculate the dose rate of both Cs-137 and Am-241, whereas equation 13 was used to calculate the dose rate of Co-60 as shown in Table 13. The dose rates and prescribed dose of each source is displayed in Table 13 in the format that is written for simplicity of calculating the time that was set on the irradiator when irradiating the RPLGDs.

Table 13: Source dose rates.

Radiation source	Co-60 source	Cs-137 source	Am-241 source
Dose rate (\bar{D})	$8.9749E+02$ (mGy/min)	$878.4976E-05$ (mGy/sec)	$64.15952E-02$ ($\mu\text{Gy/sec}$)

4.6 Irradiation time results

Equation 14 was used to calculate irradiation times of the glass dosimeters. Irradiation times of each sources with corresponding prescribed doses are indicated in Table 14. The reference prescribed doses and the corresponding irradiation times are highlighted in bold for each source.

Table 14: Irradiation times and corresponding prescribed doses.

Co-60		Cs-137		Am-241	
T _{irr} (min)	D _{pre} (mGy)	T _{irr} (sec)	D _{pre} (mGy)	T _{irr} (sec)	D _{pre} (μGy)
0.22	200	1138.3	10	866	20
0.56	500	1707.5	15	1732	40
0.89	800	2276.6	20	2598	60
1.11	1000	2845.8	25	3464	80
1.67	1500	3414.9	30	4329	100
2.23	2000	3984.1	35	5198	120
3.34	3000	4553.2	40	6061	140
5.57	5000				
7.80	7000				
10.03	9000				

4.7 Radiation counts acquired by RPLGD

Figures 21, 22 and 23 illustrate radiation counts for ⁶⁰Co, ¹³⁷Cs and ²⁴¹Am sources against prescribed doses. The glass dosimeters were irradiated with prescribed doses shown in Table 14 and the radiation counts the glass dosimeters acquired at the specified irradiation time are related to the prescribed doses.

4.7.1 Co-60 source radiation counts

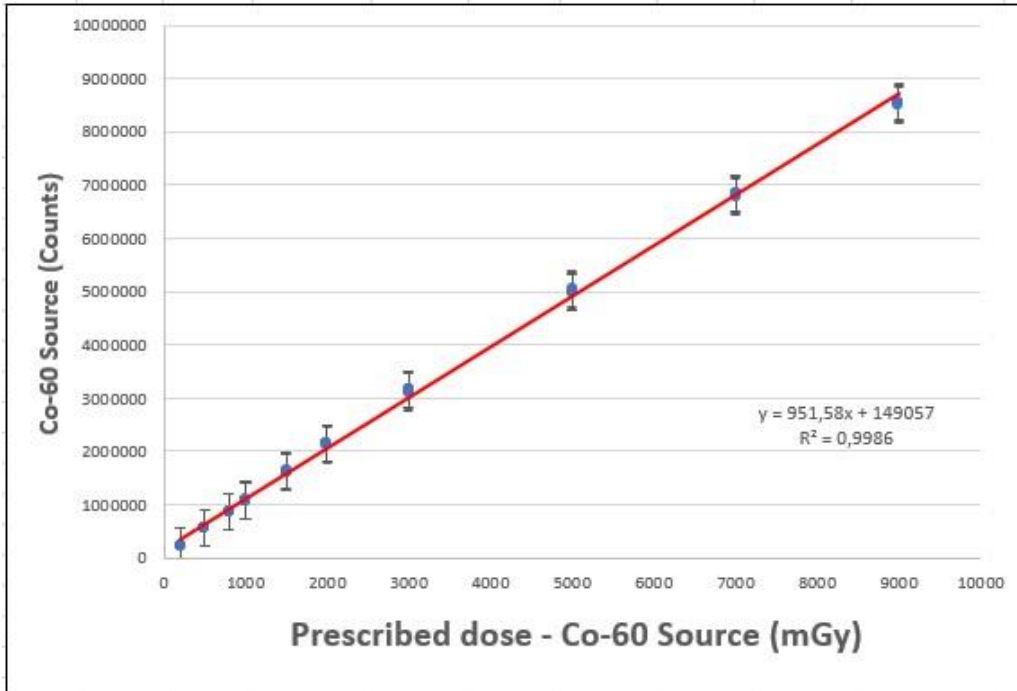


Figure 21: Co-60 source irradiation counts measured by RPLGD.

4.7.2 Cs-137 source radiation counts

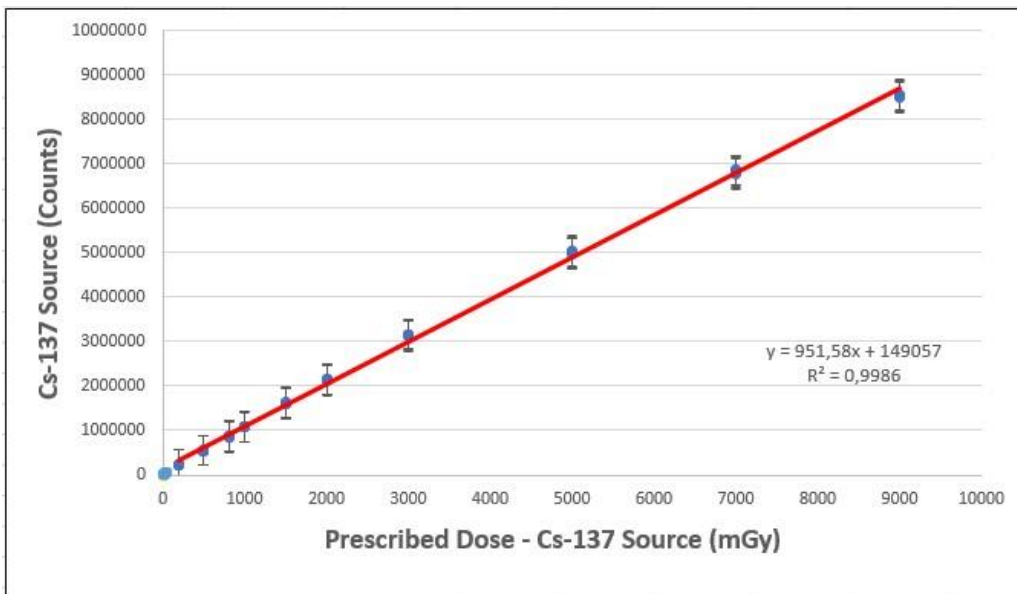


Figure 22: Cs-137 source irradiation counts measured by RPLGD.

4.7.3 Am-241 source radiation counts

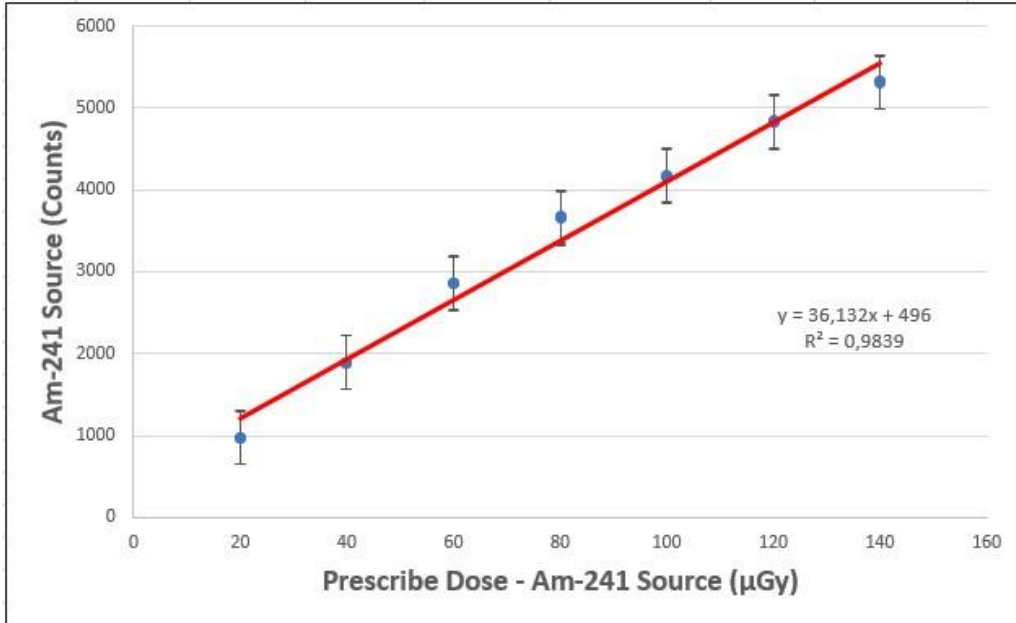


Figure 23: Am-241 source irradiation counts measured by RPLGD.

4.8 Sensitivity Correction Factors of RPLGD

Sensitivity correction factors for of glass dosimeters for all three radiation sources are shown in Figure 24 to 26.

4.8.1 Sensitivity correction factors of RPLGD in Co-60 source

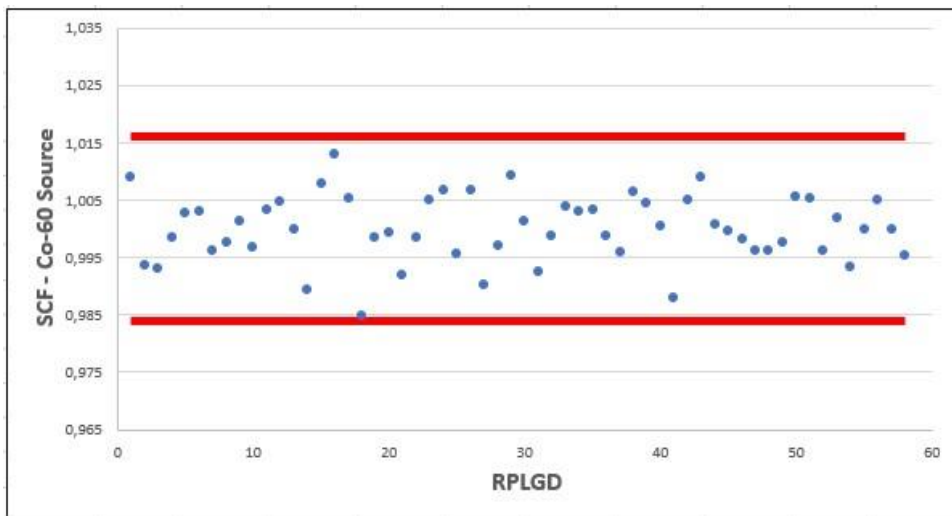


Figure 24: Sensitivity correction factors of RPLGD in Co-60 beam.

The sensitivity correction factor f_{SCF} (^{60}Co) of the 58 individual glass dosimeters irradiated in a ^{60}Co beam is shown in Figure 24. The tolerance limits of the f_{SCF} (^{60}Co) was calculated to be $\pm 1.60\%$.

4.8.2 Sensitivity correction factors of RPLGD in Cs-137 source

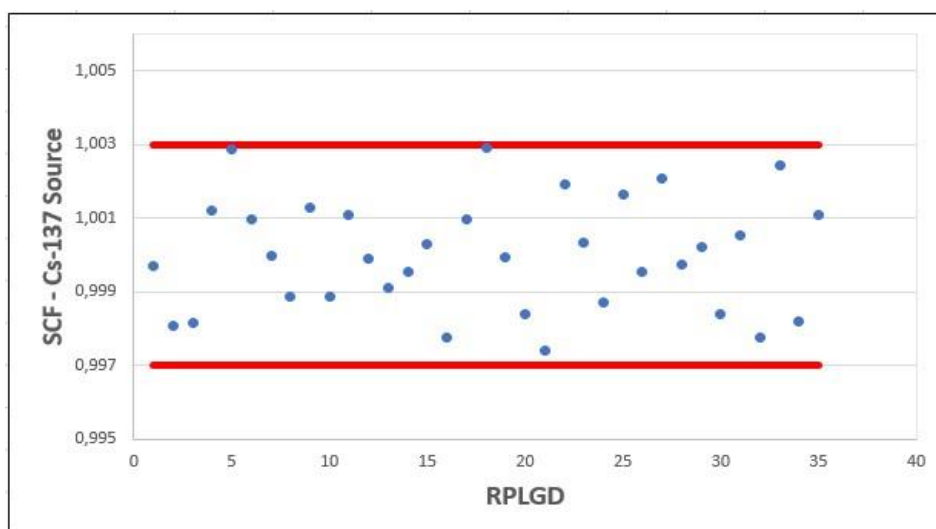


Figure 25: Sensitivity correction factors of RPLGD in Cs-137 beam.

The sensitivity correction factor f_{SCF} (^{137}Cs) of the 35 individual glass dosimeters irradiated in a ^{137}Cs beam is shown in Figure 25. The tolerance limits of the f_{SCF} (^{137}Cs) was calculated to be $\pm 0.3\%$.

4.8.3 Sensitivity Correction Factors of RPLGD in Am-241 source

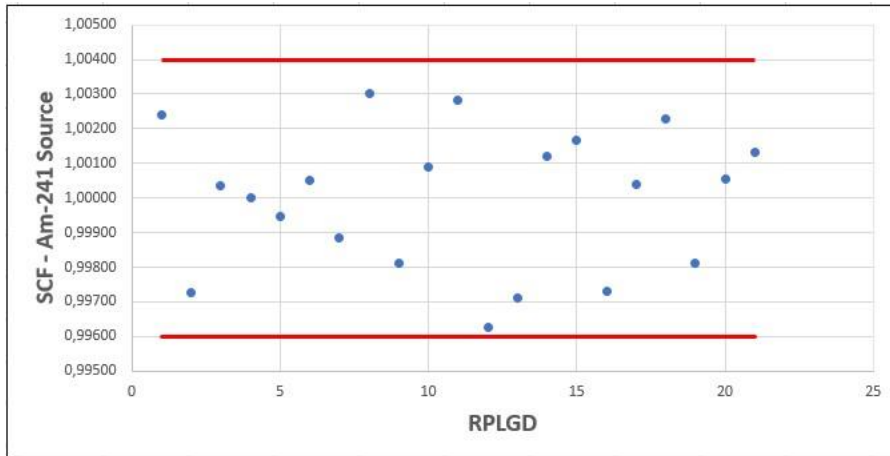


Figure 26: Sensitivity correction factors of RPLGD in Am-241 beam.

The sensitivity correction factor f_{SCF} (^{241}Am) of the 21 individual glass dosimeters irradiated in a ^{241}Am beam is shown in Figure 26. The tolerance limits of the f_{SCF} (^{241}Am) was calculated to be $\pm 0.4\%$.

4.9 RPLGD calibration coefficients

Equation 17, 18 and 19 were used to calculate the calibration coefficients (N_{RPLGD}) of the glass dosimeters for ^{60}Co , ^{137}Cs and ^{241}Am sources.

4.9.1 RPLGD calibration coefficient for Co-60 source

Calibration coefficient for Co-60 is shown in Table 15.

Table 15: RPLGD calibration coefficient in ^{60}Co source.

#	Counts
1	2123927

2	2136927
3	2147928
4	2145925
5	2146928
6	2136926
$\bar{M}_{2000 \text{ mGy}}$	2139760.167

The reference radiation dose for ^{60}Co source was taken as 2000 mGy at 100 cm from the source.

$$N_{RPLGD} (Co60) = \frac{2000 \text{ mGy}}{2139760.167 \text{ counts}}$$

$$= 9.34684E -04 \text{ mGy/counts.}$$

4.9.2 RPLGD calibration coefficient for Cs-137 source

Calibration coefficient for Cs-137 is shown in Table 16.

Table 16: RPLGD calibration coefficient in ^{137}Cs source.

#	Counts
1	25146

2	25116
3	25096
4	25107
5	25126
$\bar{M}_{20 \text{ mGy}}$	25118.2

The reference radiation dose for ^{137}Cs source was taken as 20 mGy at 200 cm from the source.

$$N_{RPLGD} (Cs137) = \frac{20 \text{ mGy}}{25118.2 \text{ Counts}}$$

$$= 796.2354E -06 \text{ mGy/counts.}$$

4.9.3 RPLGD calibration coefficient for Am-241 source

Calibration coefficient for Am-241 is shown in Table 17.

Table 17: RPLGD calibration coefficient in ^{241}Am source.

#	Counts
1	975
2	970

3	973
$\bar{M}_{20 \mu\text{Gy}}$	972.66667

The reference radiation dose for ^{60}Co source was taken as 20 μGy at 50 cm from the source.

$$\begin{aligned}
 N_{RPLGD} (Am241) &= \frac{241 \mu\text{Gy}}{972.66667 \text{ counts}} \\
 &= 972.66667 \mu\text{Gy}/\text{counts} \\
 &= 205.62029E -04 \mu\text{Gy}/\text{counts}.
 \end{aligned}$$

4.10 Linearity correction factors for RPLGD

Non-linearity correction factors are shown in Figures 27, 29 and 31 below. The radiation counts are normalized at the reference dose; 2 000 mGy for ^{60}Co , 20 mGy for ^{137}Cs and 20 μGy for ^{241}Am source to determine non-linearity corrections. The non-linearity correction factors are calculated by equation 26, 27 and 28.

Linearity correction factors are calculated from the inverse of the non-linearity correction factors. To show the relationship of the prescribed dose as it increases how does it relate with the radiation counts in a linear form, linearity corrections were applied to quantify the absorbed dose of the glass dosimeter with prescribed dose. Linearity correct factors are depicted in Figure 28, 30 and 32.

4.10.1 Linearity correction factors for RPLGD in Co-60 source

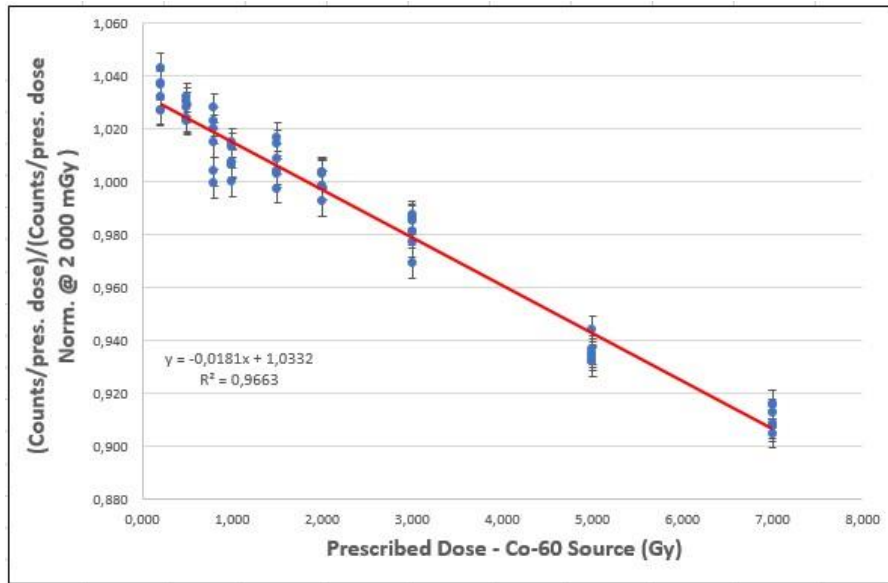


Figure 27: Non-linearity coefficients of RPLGD in ^{60}Co beam.

$$f_{non-lin} = -0.0181x + 1.0332 \quad (26)$$

Where x is the prescribed dose (mGy) given to the glass dosimeters.

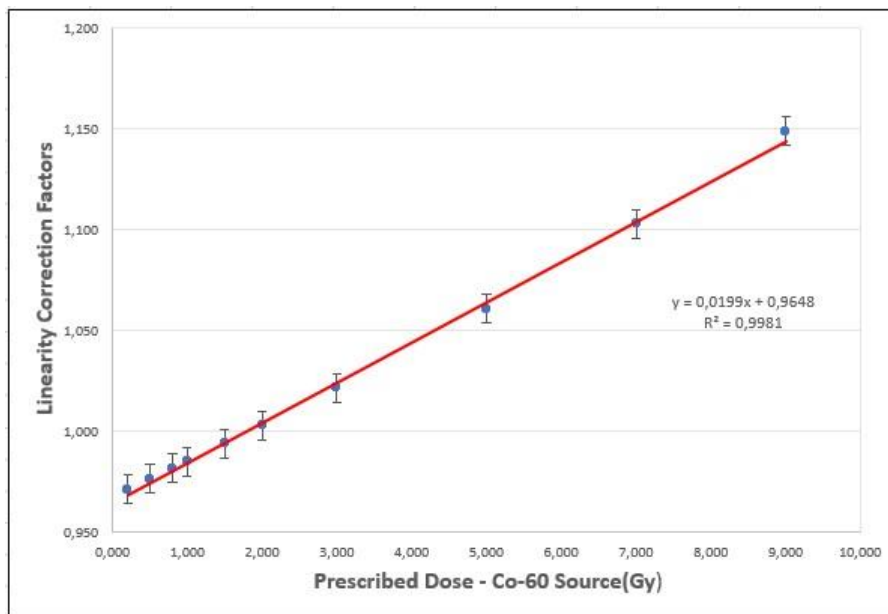


Figure 28: Linearity correction factors of RPLGD in ^{60}Co beam.

Linearity correction factors for glass dosimeters in ^{60}Co source shows linear response when the prescribed dose increases with time. The R^2 value is 99.81 % which shows a variance on the radiation counts of 0.19 %, which is a good evidence of the linearity response.

4.10.2 Linearity correction factors for RPLGD in Cs-137 source

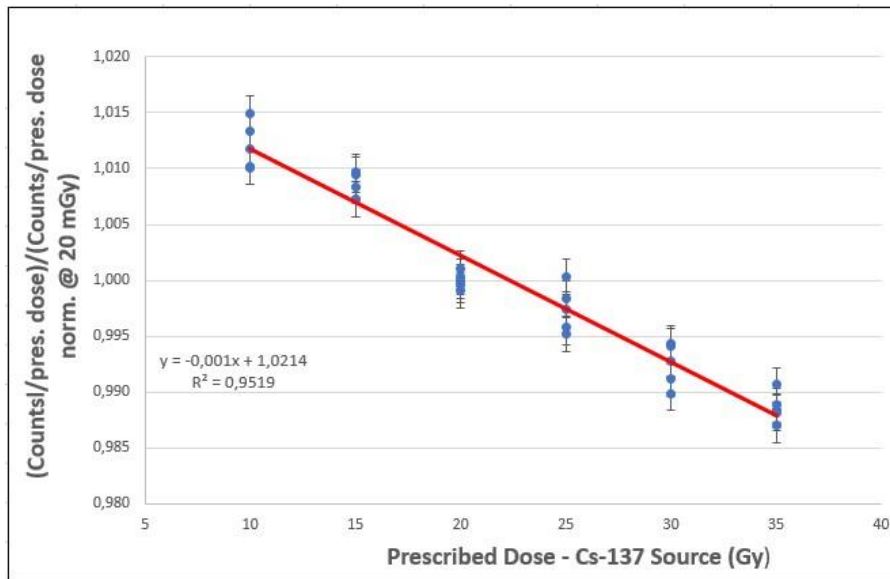


Figure 29: Non-linearity coefficients of RPLGD in ^{137}Cs beam.

$$f_{non-lin} = -0.001x + 1.0214 \quad (27)$$

Where x is the prescribed dose (mGy) given to the glass dosimeters.

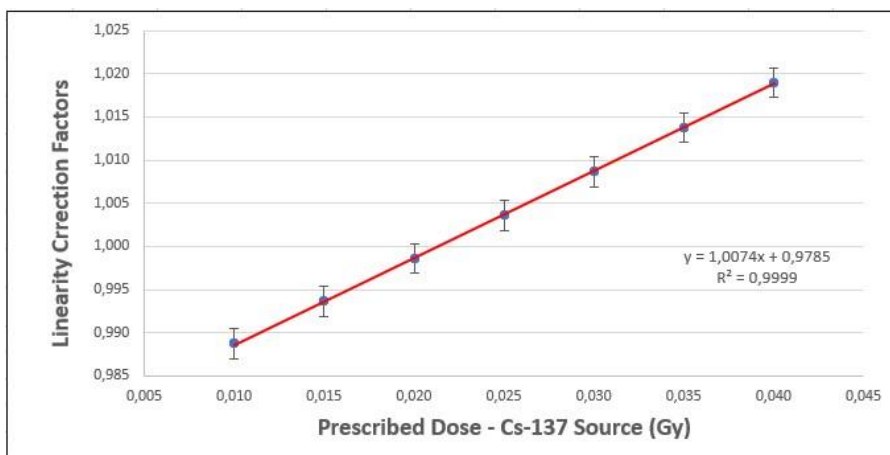


Figure 30: Linearity correction factors of RPLGD in ^{137}Cs beam.

Linearity correction factors for glass dosimeters in ^{137}Cs source shows linear response when the prescribed dose increases with time. The R^2 value is 99.99 % which shows a variance on the radiation counts of 0.11 %, which is almost 100 % evidence of the linearity response.

4.10.3 Linearity correction factors for RPLGD in Am-241 source

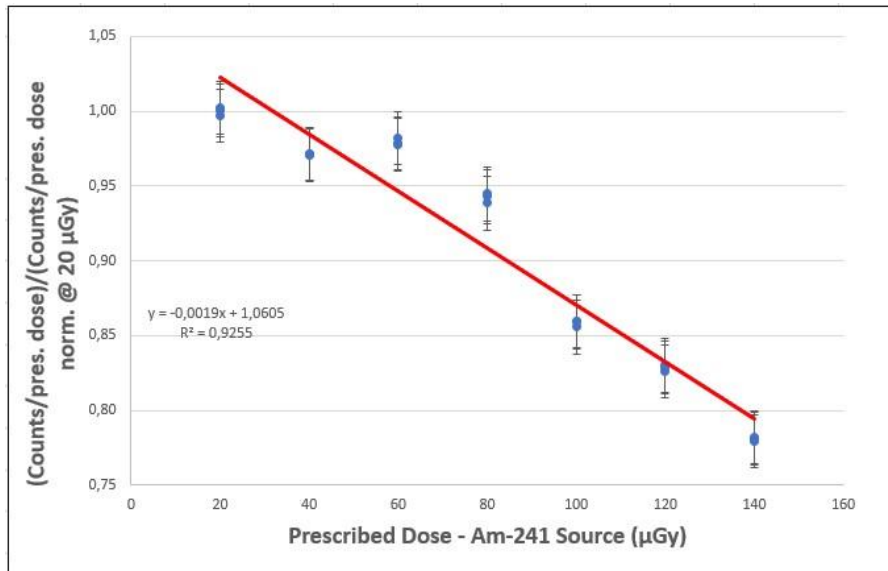


Figure 31: Non-linearity coefficients of RPLGD in ^{241}Am beam.

$$f_{non-lin} = -0.0019x + 1.0602 \quad (28)$$

Where x is the prescribed dose (μGy) given to the glass dosimeters.

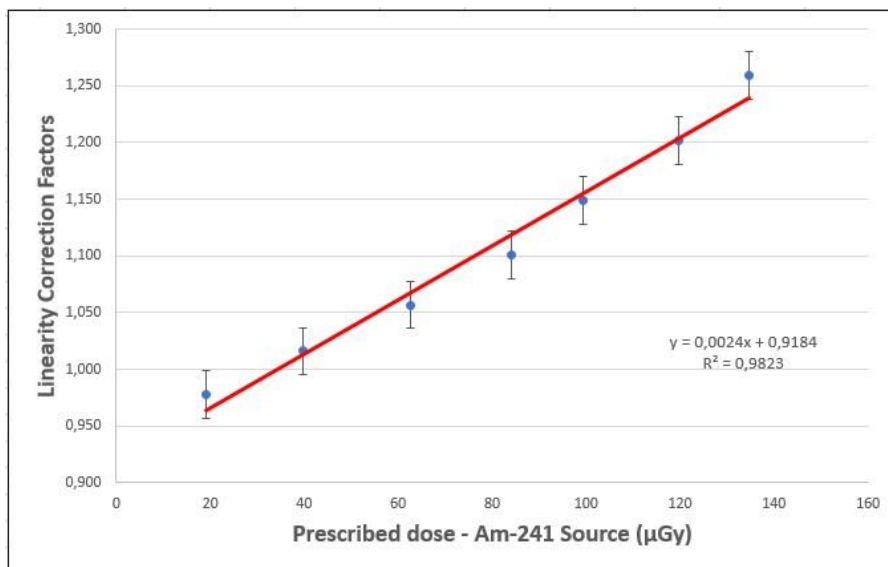


Figure 32: Linearity correction factors of RPLGD in ^{241}Am beam.

Linearity correction factors for glass dosimeters in ^{241}Am source shows linear response when the prescribed dose increases with time. The R^2 value is 98.23 % which shows a variance on the radiation counts of 1.77 %, which is a good evidence of the linearity response.

4.11 RPLGD corrected radiation counts - absorbed dose

Tables 18, 19 and 20 shows the prescribed doses delivered to the glass dosimeters, with corresponding uncorrected radiation counts acquired and the absorbed doses of the glass dosimeter after the corrections of the radiation counts. Figures 33 to 35 depict the calculated absorbed dose of glass dosimeters in three radiation sources.

4.11.1 RPLGD Absorbed dose in Co-60 beam

Table 18: Corrected radiation counts by Co-60 source.

Prescribed Dose (mGy)	200	500	800	1000	1500	2000	3000	5000	7000	9000
Radiation Counts	221244	549378	868628	1078595	1616928	2139760	3148927	5004594	6820594	8527174
Absorbed dose (mGy)	199	507	802	977	1520	2019	2972	4999	7109	9147
Time (min)	0,22	0,56	0,89	1,11	1,67	2,23	3,34	5,57	7,80	10,03
% difference	-0,4	1,4	0,2	-2,3	1,3	1,0	-0,9	0,0	1,6	1,6

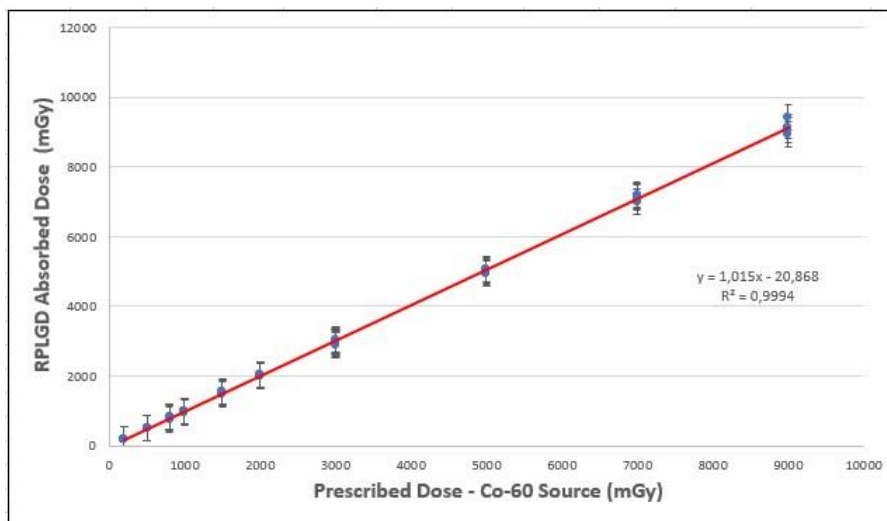


Figure 33: Absorbed dose by RPLGD in ^{60}Co source.

The individual percentage difference that was calculated for absorbed dose to that of the prescribed dose make a maximum of 5.3 % whereas the average glass dosimeters has a maximum of 1.6 % which was obtained from equation 21 as indicated in Tables 20 and 21 on annexure 2. The value of $R^2 = 99.94$ % confirms a small difference on the prescribed radiation dose delivered to the glass dosimeters and the absorbed dose measured. At this stage, it is safe to claim that the glass dosimeter can be used as the personal dosimeter and the radiation monitoring instrument for gamma radiation in ^{60}Co source.

4.11.2 RPLGD Absorbed dose in Cs-137 beam

Table 19: Corrected radiation counts by Cs-137 source.

Prescribed Dose (mGy)	10	15	20	25	30	35	40
Radiation Counts	12711	18997	25118	31316	37394	43456	50699
Absorbed dose (mGy)	9,92	15,18	20,13	24,90	29,76	35,43	41,46
Time (sec)	1138,3	1707,5	2276,6	2845,8	3414,9	3984,1	4553,2
% difference	-0,8	1,2	0,7	-0,4	-0,8	1,2	3,7

Similarly, ^{137}Cs source measurements results follows the same pattern of response as the ^{60}Co source. The maximum percentage difference of the individual glass dosimeters of 4.1 % whereas the

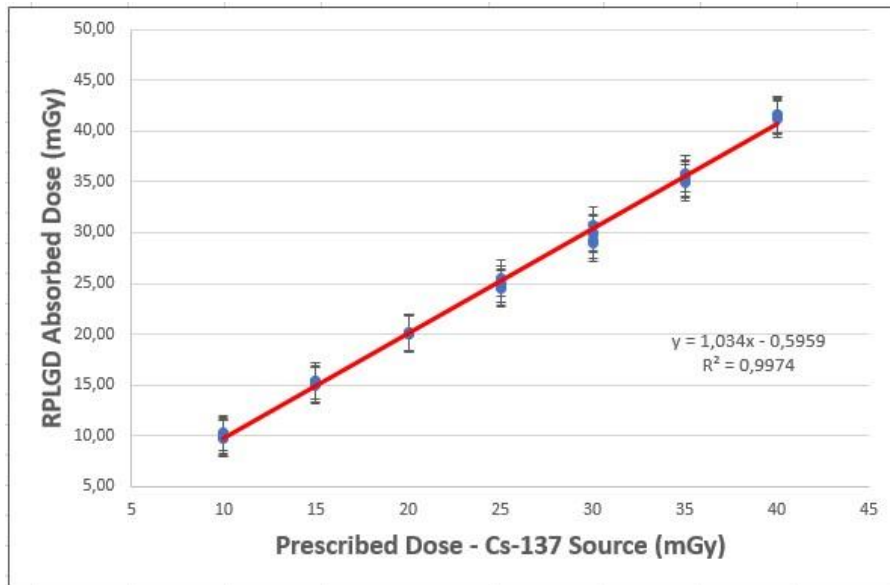


Figure 34: Absorbed dose by RPLGD in ^{137}Cs source.

average glass dosimeters have a maximum of 3.7 % which was obtained from equation 21 as well as indicated in Table 22 and annexure 3. The value of $R^2 = 99.74 \%$ confirms a small difference on the prescribed radiation dose delivered to the glass dosimeters to the absorbed dose measured. The ^{137}Cs source measurements for absorbed dose in comparisons with the prescribed dose of the glass dosimeter can be used as the personal dosimeter and the radiation monitoring instrument for gamma radiation.

4.11.3 RPLGD absorbed dose in Am-241 beam

Table 20: Corrected radiation counts by Am-241 source.

Prescribed Dose (μGy)	20,0	40,0	60,0	80,0	100,0	120,0	140,0
Radiation Counts	973	1889	2857	3665	4173	4833	5316
Absorbed dose (μGy)	19,1	39,7	62,7	84,1	99,4	119,8	134,6
Time (sec)	866	1732	2598	3464	4329	5195	6061
% difference	-4,3	-0,8	4,5	5,1	-0,6	-0,2	-3,8

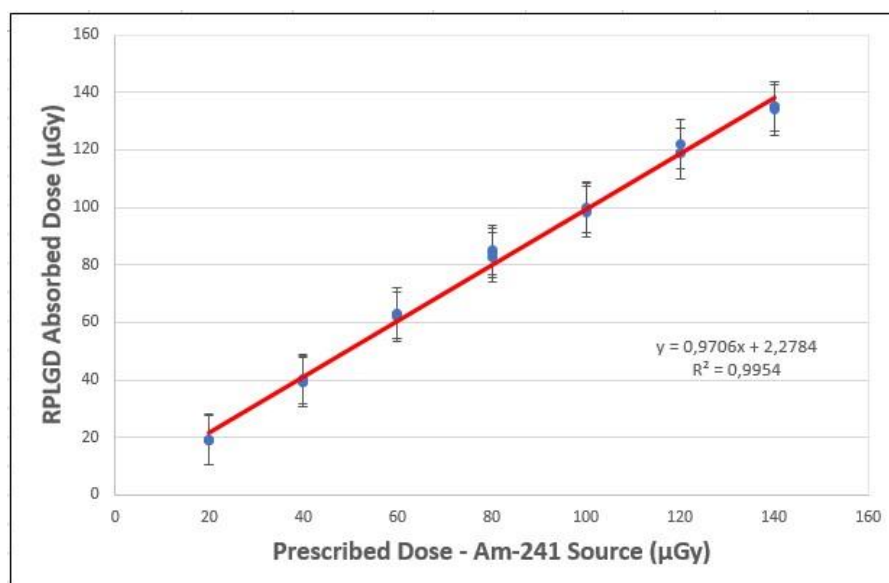


Figure 35: Absorbed dose by RPLGD in ^{241}Am source.

he ^{241}Am source measurements results also are in similar response with the other two sources (i.e. ^{137}Cs and ^{60}Co source). The maximum percentage difference of the individual glass dosimeters of 6.5 % whereas the average glass dosimeters has a maximum of 5.1 % which was obtained from equation 21 as well as indicated in Table 25 in Annexure 4. The value of $R^2 = 99.54\%$ confirms a small difference on the prescribed radiation dose delivered to the glass dosimeters to the absorbed dose measured.

5 CHAPTER 5: CONCLUSION

Characterization of radio-photoluminescence glass dosimeters was aimed at quantifying the response of the glass dosimeters when exposed to gamma radiation in the form of Co-60, Cs-137 and Am-241. Thus, this study emanated from the use of thermoluminescence dosimeters which is widely used by radiation workers in South Africa as instituted by South African Health Products Regulatory Authority to ensure that all radiation workers are monitored as they use radiation sources on their work activities.

Thus, the challenges which TLDs have as the primary radiation monitoring device for radiation personal monitoring and in some instances used as environmental monitoring device is its inability of being re-read for accumulated radiation signal acquired. In addressing the challenge for the TLDs, a more reliable and Table radiation detectors was used as a reference detector (i.e. spherical and farmer chamber).

Traceability of the reference measurements were drawn from the calibration coefficients of the ionization chambers. It was disseminated to the reference measurements which were used for characterization of the glass dosimeters in the measurements of air kerma and absorbed dose to water. Reference detectors were used to determine the dose rates at the reference distance and to calculate the corresponding times for irradiating the glass. The substitution method was used between the reference detectors and the unit under test (i.e. ionization chambers and the glass dosimeters under the same conditions).

Absorbed dose calculated for radio-photoluminescence glass dosimeters as opposed to the prescribed dose for Co-60 has a maximum percentage difference of 4.8 %, Cs-137 of 4.1 % and 6.5 %. The percentage difference is used as a measure to check how far the instrument reading (i.e. RPLGD readings) is to the true readings (i.e. ionization chamber readings). Thus, the intensity of the radiation source might have the significance in the lower measurements readings as is has been noted that for Am-241 source, the readings shows higher percentage difference that Co-60 and C-137 source.

The results as summarized in Annexure 1 to 4 shows when the glass dosimeters are exposed to different radiation doses using different radiation sources, the correction factors that are applied for all the parameters that have significance influence on the final measurements results are in close

agreement with the prescribed doses. Based on the results obtained, radio-photoluminescence glass dosimeters were successfully characterized with Co-60, Cs-137 and Am-241 and reference air kerma and absorbed dose to water measurements were established. The response of the glass dosimeters for the three sources varies linearly with prescribed dose". The linearity response of the glass dosimeters for the three sources, indicates that the increase in the radiation exposure or irradiation of the glass dosimeters follows the linear response on the accumulated dose as indicated by the glass dosimeter's readings shown in Table 22 to 25. Thus, the calibration coefficient for the three radiation sources can be easily applied to the reference measurements to obtain any desired measurements be it personal dose equivalent rate (personal monitoring) or ambient dose equivalent (environmental monitoring).

The aim of the study which was to quantify or characterize the glass dosimeter response with three radiation sources has been achieved, the results are evidence. Further future studies on the glass dosimeters was to determine the energy dependence of the glass dosimeters, measurements on the fading effect, depletion and the uncertainty contributors. Finally, it suffices to conclude with confidence drawn from the results obtained, that the radio-photoluminescence glass dosimeters are capable of being re-read multiple times without losing any signal.

5.1 Annexure 1

Table 21: Magazine correction factors.

Position	Actual data	Curve fit
1	0,970	0,970
2	0,990	0,980
3	0,975	0,985
4	1,000	0,995
5	1,015	1,000
6	0,995	1,005
7	1,000	1,005
8	1,010	1,010
9	1,020	1,010
10	1,025	1,015
11	1,005	1,015
12	1,005	1,010
13	1,005	1,010
14	1,010	1,010
15	1,010	1,005
16	1,000	1,005
17	1,020	1,000
18	0,990	0,995
19	0,985	0,990
20	0,980	0,985

5.2 Annexure 2

Table 22: Co-60 results.

No.	Radiation Counts	Magazine Correction Factors	Sensitivity Correction Factors	Prescribed Dose (mGy)	Counts/ Prescribed Dose (mGy)	Counts/ Prescribed Dose (mGy)/ (norm. to 2 000 mGy)	Prescribed Dose (Gy)	Non Linearity Correction Factors	Linearity Correction Factors	Absorbed Dose (mGy)	% Difference
1	223227	0,970	1,0089630	200	1116,1350	1,0432337	0,200	1,02958	0,9712698	198	0,8
2	219828	0,990	0,9935998	200	1099,1400	1,0273488	0,200	1,02958	0,9712698	196	1,8
3	219728	0,975	0,9931478	200	1098,6400	1,0268814	0,200	1,02958	0,9712698	193	3,4
4	220928	1,000	0,9985717	200	1104,6400	1,0324895	0,200	1,02958	0,9712698	200	0,1
5	221826	1,020	1,0026306	200	1109,1300	1,0366863	0,200	1,02958	0,9712698	206	3,0
6	221927	0,995	1,0030871	200	1109,6350	1,0371583	0,200	1,02958	0,9712698	201	0,5
7	547328	1,000	0,9962691	500	1094,6560	1,0231577	0,200	1,02415	0,9764195	498	0,5
8	548029	1,010	0,9975451	500	1096,0580	1,0244681	0,200	1,02415	0,9764195	504	0,8
9	550028	1,020	1,0011838	500	1100,0560	1,0282050	0,200	1,02415	0,9764195	513	2,5
10	547627	1,025	0,9968134	500	1095,2540	1,0237166	0,200	1,02415	0,9764195	511	2,1
11	551227	1,010	1,0033662	500	1102,4540	1,0304463	0,200	1,02415	0,9764195	510	2,0
12	552027	1,005	1,0048224	500	1104,0540	1,0319418	0,200	1,02415	0,9764195	509	1,8
13	868627	1,005	0,9999990	800	1085,7838	1,0148649	0,200	1,01872	0,981624	801	0,1
14	859429	1,010	0,9894099	800	1074,2863	1,0041184	0,200	1,01872	0,981624	788	1,5
15	875427	1,010	1,0078275	800	1094,2838	1,0228097	0,200	1,01872	0,981624	818	2,2
16	879828	1,000	1,0128941	800	1099,7850	1,0279517	0,200	1,01872	0,981624	818	2,2
17	873128	1,020	1,0051808	800	1091,4100	1,0201237	0,200	1,01872	0,981624	821	2,7
18	855328	0,990	0,9846887	800	1069,1600	0,9993269	0,200	1,01872	0,981624	765	4,4
19	1076934	0,985	0,9984600	1000	1076,9340	1,0065932	0,200	1,0151	0,9851246	975	2,5
20	1077929	0,980	0,9993825	1000	1077,9290	1,0075232	0,200	1,0151	0,9851246	972	2,8
21	1069926	0,970	0,9919627	1000	1069,9260	1,0000429	0,200	1,0151	0,9851246	948	5,2
22	1076929	0,990	0,9984554	1000	1076,9290	1,0065885	0,200	1,0151	0,9851246	980	2,0
23	1083925	0,975	1,0049416	1000	1083,9250	1,0131276	0,200	1,0151	0,9851246	978	2,2
24	1085927	1,000	1,0067977	1000	1085,9270	1,0149988	0,200	1,0151	0,9851246	1007	0,7
25	1609930	1,020	0,9956721	1500	1073,2867	1,0031841	0,200	1,00605	0,9939864	1519	1,3
26	1627927	0,995	1,0068025	1500	1085,2847	1,0143984	0,200	1,00605	0,9939864	1515	1,0
27	1600927	1,000	0,9901042	1500	1067,2847	0,9975741	0,200	1,00605	0,9939864	1473	1,8
28	1611929	1,010	0,9969084	1500	1074,6193	1,0044297	0,200	1,00605	0,9939864	1508	0,5
29	1631927	1,020	1,0092763	1500	1087,9513	1,0168909	0,200	1,00605	0,9939864	1561	4,1
30	1618927	1,025	1,0012364	1500	1079,2847	1,0087903	0,200	1,00605	0,9939864	1544	2,9
31	2123927	1,010	0,9926005	2000	1061,9635	0,9926005	0,200	0,997	1,003009	1996	0,2
32	2136927	1,005	0,9986759	2000	1068,4635	0,9986759	0,200	0,997	1,003009	2011	0,5
33	2147928	1,005	1,0038172	2000	1073,9640	1,0038172	0,200	0,997	1,003009	2031	1,6
34	2145925	1,010	1,0028811	2000	1072,9625	1,0028811	0,200	0,997	1,003009	2038	1,9
35	2146928	1,010	1,0033498	2000	1073,4640	1,0033498	0,200	0,997	1,003009	2040	2,0
36	2136926	1,000	0,9986755	2000	1068,4630	0,9986755	0,200	0,997	1,003009	2001	0,0
37	3135927	1,020	0,9958716	3000	1045,3090	0,9770338	0,200	0,9789	1,0215548	3042	1,4
38	3168927	0,990	1,0063514	3000	1056,3090	0,9873153	0,200	0,9789	1,0215548	3015	0,5
39	3162929	0,985	1,0044466	3000	1054,3097	0,9854466	0,200	0,9789	1,0215548	2988	0,4
40	3149926	0,970	1,0003173	3000	1049,9753	0,9813953	0,200	0,9789	1,0215548	2918	2,7

Table 23: Co-60 results.

No.	Radiation Counts	Magazine Correction Factors	Sensitivity Correction Factors	Prescribed Dose (mGy)	Counts/ Prescribed Dose (mGy)	Counts/ Prescribed Dose (mGy)/ (norm. to 2 000 mGy)	Prescribed Dose (Gy)	Non Linearity Correction Factors	Linearity Correction Factors	Absorbed Dose (mGy)	% Difference
41	3110926	0,990	0,9879321	3000	1036,9753	0,9692445	0,200	0,9789	1,0215548	2905	3,2
42	3164927	0,975	1,0050811	3000	1054,9757	0,9860691	0,200	0,9789	1,0215548	2961	1,3
43	5049927	1,000	1,0090584	5000	1009,9854	0,9440174	0,200	0,9427	1,0607829	5052	1,0
44	5008926	1,020	1,0008657	5000	1001,7852	0,9363528	0,200	0,9427	1,0607829	5070	1,4
45	5001928	0,995	0,9994674	5000	1000,3856	0,9350446	0,200	0,9427	1,0607829	4932	1,4
46	4995926	1,000	0,9982681	5000	999,1852	0,9339226	0,200	0,9427	1,0607829	4945	1,1
47	4985927	1,010	0,9962701	5000	997,1854	0,9320534	0,200	0,9427	1,0607829	4974	0,5
48	4984927	1,020	0,9960703	5000	996,9854	0,9318665	0,200	0,9427	1,0607829	5022	0,4
49	6803929	1,025	0,9975567	7000	971,9899	0,9085036	0,200	0,9065	1,103144	7173	2,5
50	6858927	1,010	1,0056203	7000	979,8467	0,9158472	0,200	0,9065	1,103144	7183	2,6
51	6856928	1,005	1,0053272	7000	979,5611	0,9155803	0,200	0,9065	1,103144	7143	2,0
52	6794926	1,005	0,9962368	7000	970,7037	0,9073014	0,200	0,9065	1,103144	7015	0,2
53	6833926	1,010	1,0019547	7000	976,2751	0,9125089	0,200	0,9065	1,103144	7131	1,9
54	6774925	1,010	0,9933043	7000	967,8464	0,9046308	0,200	0,9065	1,103144	7008	0,1
55	8525925	1,000	0,9998536	9000	947,3250	0,8854497	0,200	0,8703	1,1490291	9155	1,7
56	8568924	1,020	1,0048961	9000	952,1027	0,8899153	0,200	0,8703	1,1490291	9433	4,8
57	8525924	0,990	0,9998534	9000	947,3249	0,8854496	0,200	0,8703	1,1490291	9064	0,7
58	8487922	0,985	0,9953969	9000	943,1024	0,8815029	0,200	0,8703	1,1490291	8938	0,7

5.3 Annexure 3

Table 24: Cs-137 results.

No.	Radiation counts	Magazine Correction Factors	Sensitivity Correction Factors	Prescribed dose (mGy)	Counts/ Prescribed Dose (mGy)	Counts/ Prescribed Dose (mGy)/ (norm. to 20 mGy)	Prescribed Dose (Gy)	Non Linearity Correction Factors	Linearity Correction Factors	Absorbed Dose (mGy)	% Difference
1	12707	0,970	0,999717	10,0	1270,7	1,0117763	0,010	1,0114	0,988728	9,7	3,0
2	12686	0,990	0,998065	10,0	1268,6	1,0101042	0,010	1,0114	0,988728	9,9	1,3
3	12687	0,975	0,998143	10,0	1268,7	1,0101839	0,010	1,0114	0,988728	9,7	2,8
4	12726	1,000	1,001212	10,0	1272,6	1,0132892	0,010	1,0114	0,988728	10,0	0,3
5	12747	1,020	1,002864	10,0	1274,7	1,0149613	0,010	1,0114	0,988728	10,3	2,7
6	19016	0,995	1,000979	15,0	1267,733	1,0094142	0,015	1,0064	0,993641	15,0	0,1
7	18997	1,000	0,999979	15,0	1266,467	1,0084056	0,015	1,0064	0,993641	15,0	0,2
8	18976	1,010	0,998874	15,0	1265,067	1,0072909	0,015	1,0064	0,993641	15,1	1,0
9	19022	1,020	1,001295	15,0	1268,133	1,0097327	0,015	1,0064	0,993641	15,4	2,5
10	18976	1,025	0,998874	15,0	1265,067	1,0072909	0,015	1,0064	0,993641	15,4	2,5
11	25146	1,010	1,001107	20,0	1257,3	1,0011068	0,020	1,0014	0,998602	20,2	1,1
12	25116	1,005	0,999912	20,0	1255,8	0,9999124	0,020	1,0014	0,998602	20,1	0,3
13	25096	1,005	0,999116	20,0	1254,8	0,9991162	0,020	1,0014	0,998602	20,0	0,2
14	25107	1,010	0,999554	20,0	1255,35	0,9995541	0,020	1,0014	0,998602	20,2	0,8
15	25126	1,010	1,000311	20,0	1256,3	1,0003105	0,020	1,0014	0,998602	20,2	0,9
16	31246	1,000	0,997758	25,0	1249,84	0,9951669	0,025	0,9964	1,003613	24,9	0,3
17	31347	1,020	1,000984	25,0	1253,88	0,9983836	0,025	0,9964	1,003613	25,6	2,3
18	31407	0,990	1,002899	25,0	1256,28	1,0002946	0,025	0,9964	1,003613	24,9	0,3
19	31315	0,985	0,999962	25,0	1252,6	0,9973645	0,025	0,9964	1,003613	24,6	1,4
20	31266	0,980	0,998397	25,0	1250,64	0,9958038	0,025	0,9964	1,003613	24,4	2,2
21	37297	0,970	0,997395	30,0	1243,233	0,9899064	0,030	0,9914	1,008675	29,0	3,4
22	37466	0,990	1,001915	30,0	1248,867	0,9943918	0,030	0,9914	1,008675	29,8	0,5
23	37407	0,975	1,000337	30,0	1246,9	0,9928259	0,030	0,9914	1,008675	29,3	2,3
24	37346	1,000	0,998706	30,0	1244,867	0,9912069	0,030	0,9914	1,008675	30,0	0,1
25	37456	1,020	1,001647	30,0	1248,533	0,9941264	0,030	0,9914	1,008675	30,7	2,4
26	43436	0,995	0,999544	35,0	1241,029	0,9881509	0,035	0,9864	1,013788	34,9	0,4
27	43546	1,000	1,002076	35,0	1244,171	0,9906533	0,035	0,9864	1,013788	35,2	0,6
28	43445	1,010	0,999751	35,0	1241,286	0,9883556	0,035	0,9864	1,013788	35,4	1,2
29	43466	1,020	1,000235	35,0	1241,886	0,9888334	0,035	0,9864	1,013788	35,8	2,3
30	43386	1,025	0,998394	35,0	1239,6	0,9870134	0,035	0,9864	1,013788	35,8	2,4
31	50726	1,010	1,000533	40,0	1268,15	1,0097459	0,040	0,9814	1,018953	41,6	4,0
32	50585	1,005	0,997751	40,0	1264,625	1,0069392	0,040	0,9814	1,018953	41,2	2,9
33	50822	1,005	1,002426	40,0	1270,55	1,0116569	0,040	0,9814	1,018953	41,5	3,8
34	50607	1,010	0,998185	40,0	1265,175	1,0073771	0,040	0,9814	1,018953	41,4	3,5
35	50755	1,010	1,001105	40,0	1268,875	1,0103232	0,040	0,9814	1,018953	41,6	4,1

5.4 Annexure 4

Table 25: Am-241 result.

No.	Radiation counts	Magazine Correction Factors	Sensitivity Correction Factors	Prescribed dose (μGy)	Counts/ Prescribed Dose (μGy)	Counts/ Prescribed Dose (μGy)/ (norm. to 20 μGy)	Non Linearity Correction Factors	Linearity Correction Factors	Absorbed Dose (μGy)	% Difference
1	975	0,970	1,00239890	20,0	48,750	1,002399	1,0222	0,978282	19,1	4,7
2	970	0,990	0,99725840	20,0	48,500	0,997258	1,0222	0,978282	19,3	3,7
3	973	0,975	1,00034270	20,0	48,650	1,000343	1,0222	0,978282	19,1	4,6
4	1889	1,000	1,00000000	40,0	47,225	0,971042	0,9842	1,016054	39,5	1,3
5	1888	1,020	0,99947062	40,0	47,200	0,970528	0,9842	1,016054	40,2	0,5
6	1890	0,995	1,00052938	40,0	47,250	0,971556	0,9842	1,016054	39,3	1,7
7	2854	1,000	0,99883341	60,0	47,567	0,978067	0,9462	1,056859	61,9	3,2
8	2866	1,010	1,00303313	60,0	47,767	0,98218	0,9462	1,056859	63,1	5,2
9	2852	1,020	0,99813346	60,0	47,533	0,977382	0,9462	1,056859	63,1	5,2
10	3668	1,025	1,00090959	80,0	45,850	0,942769	0,9082	1,101079	85,2	6,5
11	3675	1,010	1,00281972	80,0	45,938	0,944568	0,9082	1,101079	84,3	5,3
12	3651	1,005	0,99627069	80,0	45,638	0,9384	0,9082	1,101079	82,8	3,5
13	4161	1,005	0,99712437	100,0	41,610	0,855586	0,8702	1,149161	98,5	1,5
14	4178	1,010	1,00119818	100,0	41,780	0,859082	0,8702	1,149161	99,8	0,2
15	4180	1,010	1,00167745	100,0	41,800	0,859493	0,8702	1,149161	99,9	0,1
16	4820	1,000	0,99731016	120,0	40,167	0,825908	0,8322	1,201634	118,8	1,0
17	4835	1,020	1,00041382	120,0	40,292	0,828478	0,8322	1,201634	121,9	1,6
18	4844	0,990	1,00227602	120,0	40,367	0,830021	0,8322	1,201634	118,8	1,0
19	5306	0,985	0,99811889	140,0	37,900	0,779301	0,7942	1,259129	135,1	3,5
20	5319	0,980	1,00056433	140,0	37,993	0,78121	0,7942	1,259129	135,0	3,5
21	5323	0,970	1,00131678	140,0	38,021	0,781798	0,7942	1,259129	133,9	4,4

6 REFERENCES

- Akselroda, M., Botter-Jensen, L., & McKeever, S. (2007). Optical stimulated luminescence and its use in medical dosimetry. *Science Direct - Radiation Measurements*, 41:S78-S99.
- Andreo, P., Burns, D., Hohlfeid, K., Saiful Hug, M., Kanai, T., Laitano, F., Vynckier, S. (2006). Absorbed dose determination in external beam radiotherapy: An international code of practice for dosimetry based on standards of absorbed dose of water. 55-60.
- Attix, F. (2008). *Introduction to radiological physics and radiation dosimetry*. John Wiley and Sons.
- Bhatt, B., & Kulkarni, M. (2014). Thermoluminescent phosphors for radiation dosimetry. Trans Tech Publ.
- Botter-Jensen, L., McKeever, S., & Wintle, A. (2003). *Optical stimulated luminescence dosimetry*. Elsevier.
- Gregoire, V., & Mackie, T. (2011). State of the art on dose prescription, reporting and recording in intensity-modulated radiation therapy (ICRU report No. 83). *Cancer Radiotherapy*, 555-559.
- Hidehito, N. (1998). Photostimulated luminescence in insulators and semiconductors. *Radiation effects and defects in solids*, 311-321.
- Hooshang, N., Shuzo, U., & Dimitris, E. (2012). *Interaction of radiation with matter*. New York, United State of America: CRC press.
- Huang, D. Y., & Shing-Ming, H. (2011). *Radio-Photoluminescence Glass Dosimeter (RPLGD)*. INTECH Open Access Publisher.
- Jeong-Eun, R., Ju-Young, H., Gwe-Ya, K., Yon-Lae, K., Dong-Oh, S., & Tae-Suk, S. (2009). A comparison of the dosimetric characteristics of a glass rod dosimeter and a thermoluminescent dosimeter for mailed dosimeter. *Radiation measurements*, 18--22.
- Joanna, I., & Govinda, R. (2005). Radiation dosimeters. *Radiation oncology physics: a handbook for teachers and students.*, 71-99.
- Julian, P. (1987). *RPL Dosimetry, Radiophotoluminescence in Health Physics*. CRC Press.
- Kristina Jorkov, T. (2004). *Optically stimulated luminescence techniques in retrospective dosimetry using single grains of quartz extracted from unheated materials*. Riso National Laboratory.

- Lakowicz, J. (2013). *Principles of fluorescence spectroscopy*. Springer science & business media.
- Lee, J., Lin, M., Hsu, S., Chen, I., Chen, W., & Wang, C. (2007). Characterization of optically stimulated luminescence dosimeters, OLSDS for clinical dosimetric measurements. *Medical Physics*, 34(12).
- Lee, J., Lin, M., Hsu, S., Chen, I., Chen, W., & Wang, C. (2009). Dosimetry characteristics and performance comparisons: Environmental radiophotoluminescent glass dosimeters versus thermoluminescent dosimeters. *Radiation Measurements*, 86-91.
- LTD AGC TECHNO GLASS CO. (2008). *RPL Glass Dosimeter/ Small Element System*. AGC TECHNO GLASS CO., LTD.
- Martin, A., Harbison, S., Beach, K., & Cole, P. (2018). *An introduction to radiation protection*. CRC Press.
- Miyamoto, Y., Takei, Y., Nanto, H., Kurobori, T., Konnai, A., Yanagida, T., . . . Miura, K. (2011). Radiophotoluminescence from silver-doped phosphate glass. *Radiation Measurements*, 1480--1483.
- Nickovic, M., & Adrovic, F. (2012). Air kerma rate constants for nuclides important to gamma ray dosimetry and practical application. *Book on Demand*, 1.
- Norbert, V., Hajek, M., & Berger, T. (2013). Ambient dose equivalent $H^*(d)$ - an appropriate philosophy for radiation monitoring onboard aircraft and in space.
- Podgorsak, E. (2008). Radiation oncology physics: a handbook for teacher and students. *British journal of cancer*, 71-99.
- SANAS. (2014). Criteria for laboratory accreditation in the field of ionization radiation for radiation monitoring equipment. *TR-18-02*, pp. 3-9.
- Sato, F., Zushi, N., Nagai, T., Tanaka, T., Kato, Y., Yamamoto, T., & Lida, T. (2013). Development of radiophotoluminescence glass dosimeter usable in high temperature environment. *Radiation Measurements*, 53:8-11.
- Seco, J., Clasié, B., & Partridge, M. (2014). Review on the characteristics of radiation detectors for dosimetry and imaging. *Physics in Medicine and Biology*, R303.
- Sijun, F., Chunlei, Y., Dongbing, H., & Kefeng, L. (2011). Gamma rays induced defect centers in phosphate glass for radio-photoluminescence dosimeter. *Radiation measurements*, 46-50.

Toshio, K., Akihiro, T., Yuka, M., Daisuke, M., Yasuhiro, K., Nobuhiro, T., . . . Yao Qiang, C. (2015). A disk-type dose image detector based on blue and orange RPL in Ag-activated phosphate glass for 2D and 3D dose imaging applications. *Radiation Measurements*, 51-55.

Weihai, Z., Weiqi, L., Guoying, Z., & Gang, H. (2007). Comparisons of dosimetric properties between radiophotoluminescent glass rod detector and thermoluminescent detectors. *International Radiation Protection Association*, 40--74.

Yamamoto, T. (2011). Rpl dosimetry: Principles and applications. *In AIP Conference Proceedings* (pp. 217-230). AIP.

Yohei, I., Atsuya, K., Wataru, K., Fuminobu, S., Yushi, K., Takayoshi, Y., & Toshiyuki, I. (2008). A compact system for measurement of radiophotoluminescence of phosphate glass dosimeter. *Radiation measurements*, 542-545.